



# Remembering Aron Pinczuk: My Friend and Collaborator

Jainendra Jain, October 8, 2022

JUN 15 2007



**Light scattering brought us together.**

**Our friendship led to much fruitful collaboration.**



**June 2007 EPQHS Penn State**



**June 2007 EPQHS Penn State**



**October 2016 EP2DS Penn State**



**August 2017 EP2DS Penn State**

# **Raman scattering from layered electron gas**

**My entry into physics research**

# Plasma dispersion in a layered electron gas: A determination in GaAs-(AlGa)As heterostructures

Diego Olego and A. Pinczuk

*Bell Laboratories, Holmdel, New Jersey 07733*

A. C. Gossard and W. Wiegmann

*Bell Laboratories, Murray Hill, New Jersey 07974*

(Received 30 April 1982)

The dispersion of the plasma frequency of layered electron gases in GaAs-(AlGa)As heterostructures was determined by inelastic light scattering. The measured dispersions differ from that in two- and three-dimensional plasmas. They are *linear* in the in-plane component of the wave vector. This observation confirms predictions of theoretical models.

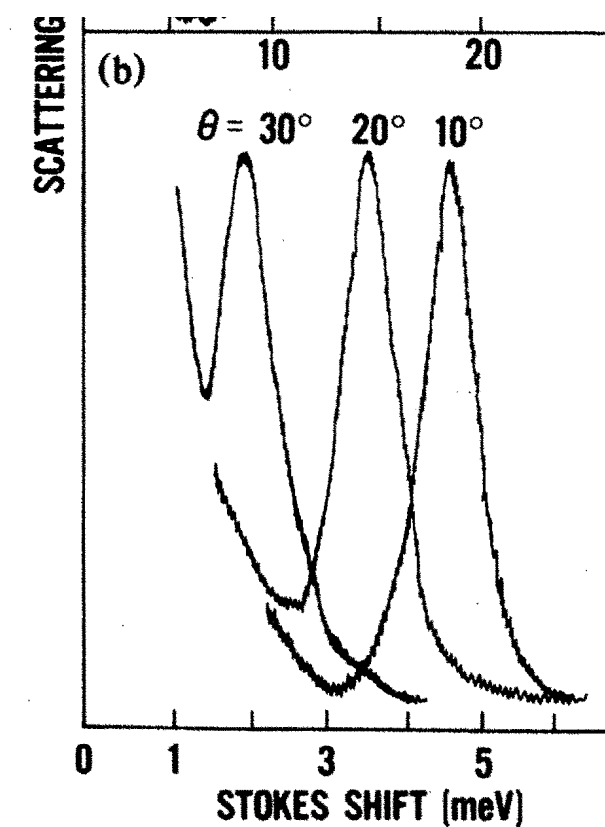


FIG. 2. (a) Typical light scattering spectra from sample 1. The low-energy band is the layered electron gas plasmon. (b) Plasmon lines of the layered electron gas for different angles  $\theta$ . With increasing  $\theta$  (decreasing  $k_{\parallel}$ ) the plasmon band shifts to lower energies.

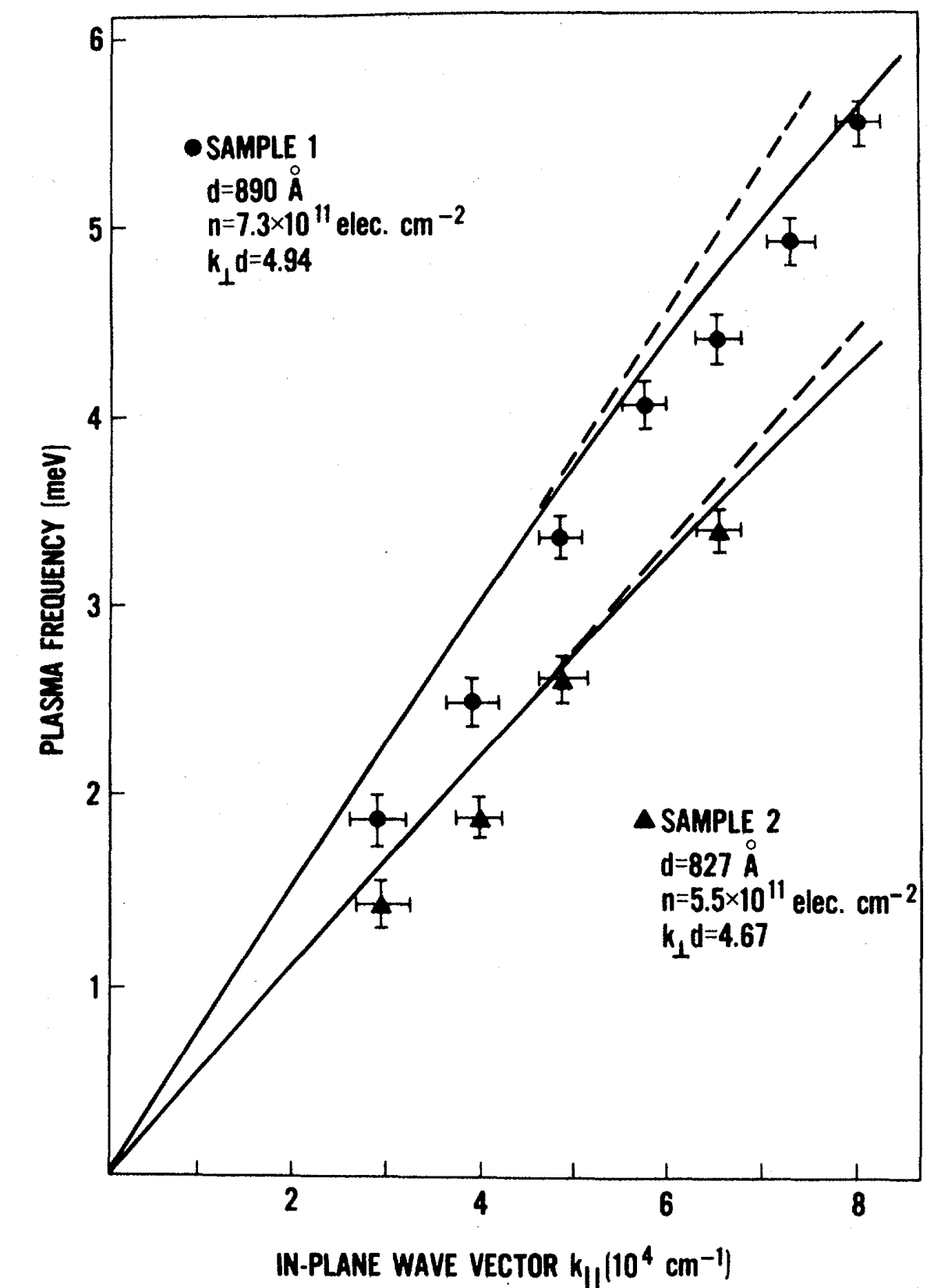


FIG. 3. Dispersion relations of the plasma frequency of the layered electron gas in the two samples. The solid lines represent the calculated dispersions with Eq. (1). The dashed lines are evaluations of Eq. (2).

$$\omega_p = k_{\parallel} \left( \frac{2\pi n e^2}{\epsilon_M m^*} \frac{d}{1 - \cos k_{\perp} d} \right)^{1/2}$$

# Dielectric response of a semi-infinite layered electron gas and Raman scattering from its bulk and surface plasmons

Jainendra K. Jain and Philip B. Allen

Department of Physics, State University of New York, Stony Brook, New York 11794

(Received 22 March 1985)

An exact solution of the random-phase-approximation equations is worked out for the density-density correlation function of a semi-infinite system of two-dimensional electron-gas layers, with different dielectrics outside and inside the layered system. From this solution, analytic formulas are derived for the dispersion relations of the bulk and surface plasmons and for the intensity of the light scattered inelastically from such a system. The intensity is written as a sum of the bulk and the surface terms. The theory is applied to semiconductor multilayers. The line shape of the bulk-plasmon peak, obtained after cancellation of van Hove singularities in the bulk piece by the surface piece, is compared with experiment. Conditions for observation of the Giuliani-Quinn surface plasmon are outlined.

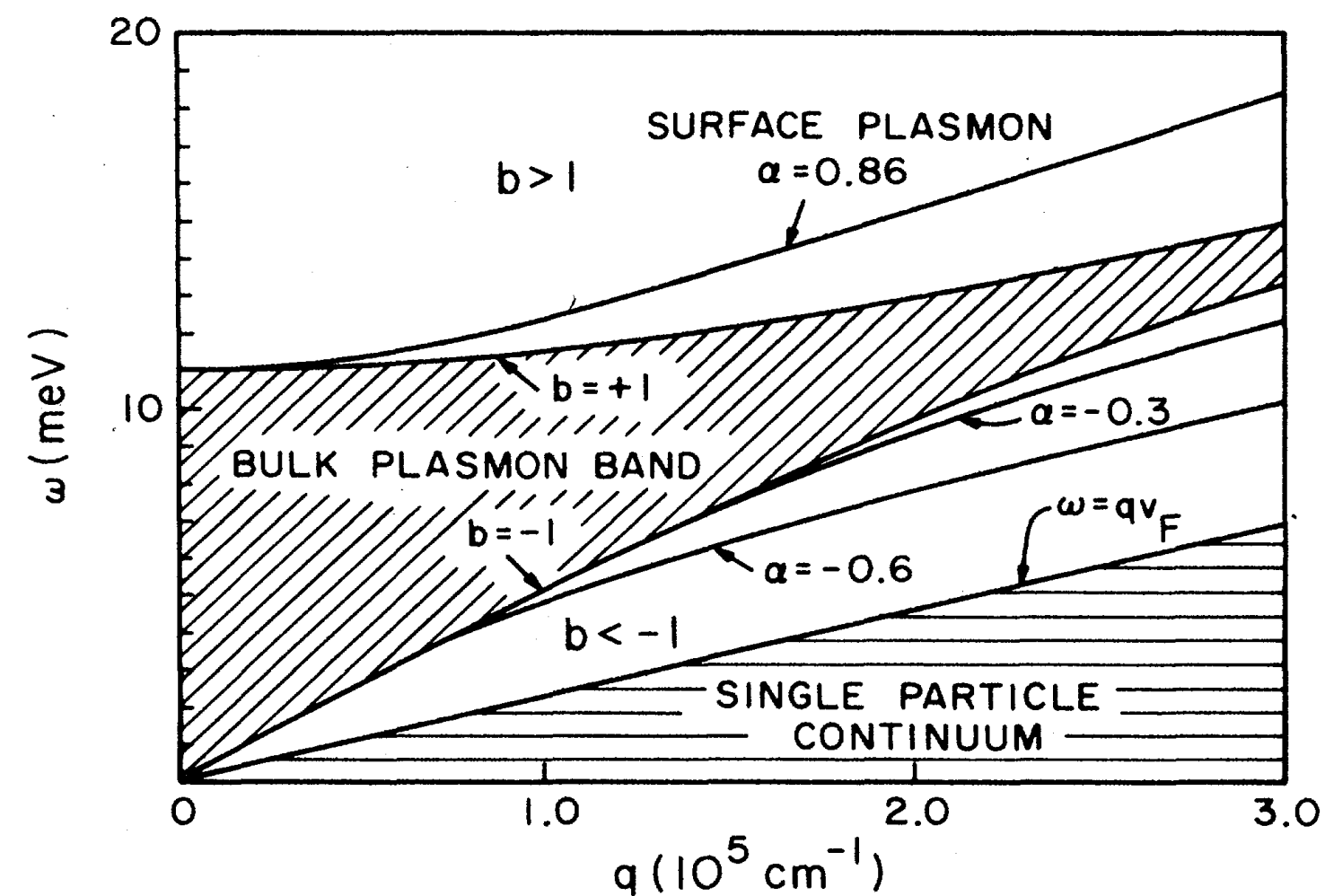


FIG. 3. Dispersion relation for the surface plasmon for certain values of  $\alpha$ . The shaded region is the bulk-plasmon band and has no surface plasmon inside it.  $\alpha=0.86$  corresponds to vacuum outside the semi-infinite LEG.

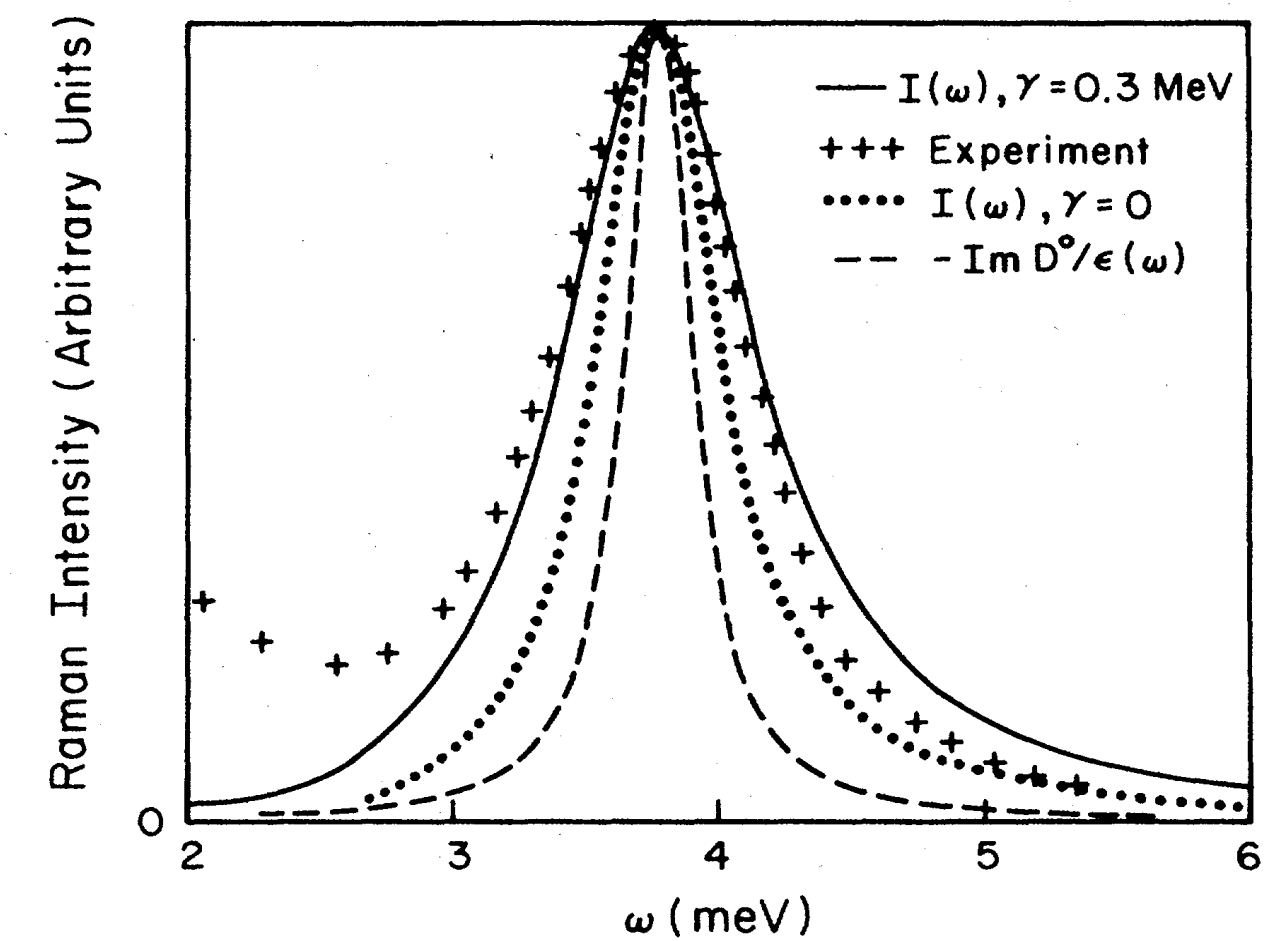


FIG. 4. Comparison between the experimental and theoretical line shapes of the bulk-plasmon peak in the Raman spectrum. The experimental peak has been shifted along the  $\omega$  axis to align it with the other peak. The result of a naive theory  $I(\omega) = -\text{Im } D^0/\epsilon(\omega)$  is also shown. All the spectra are normalized separately.

## Plasmons in Layered Films

Jainendra K. Jain and Philip B. Allen

*Department of Physics, State University of New York, Stony Brook, New York 11794*

(Received 3 April 1985)

A random-phase-approximation theory is given for the electronic collective modes of a film containing  $N$  equally spaced layers of two-dimensional electron gas. Raman line shapes are predicted. The Giuliani-Quinn surface-plasmon intensity is enhanced in transmission geometry.

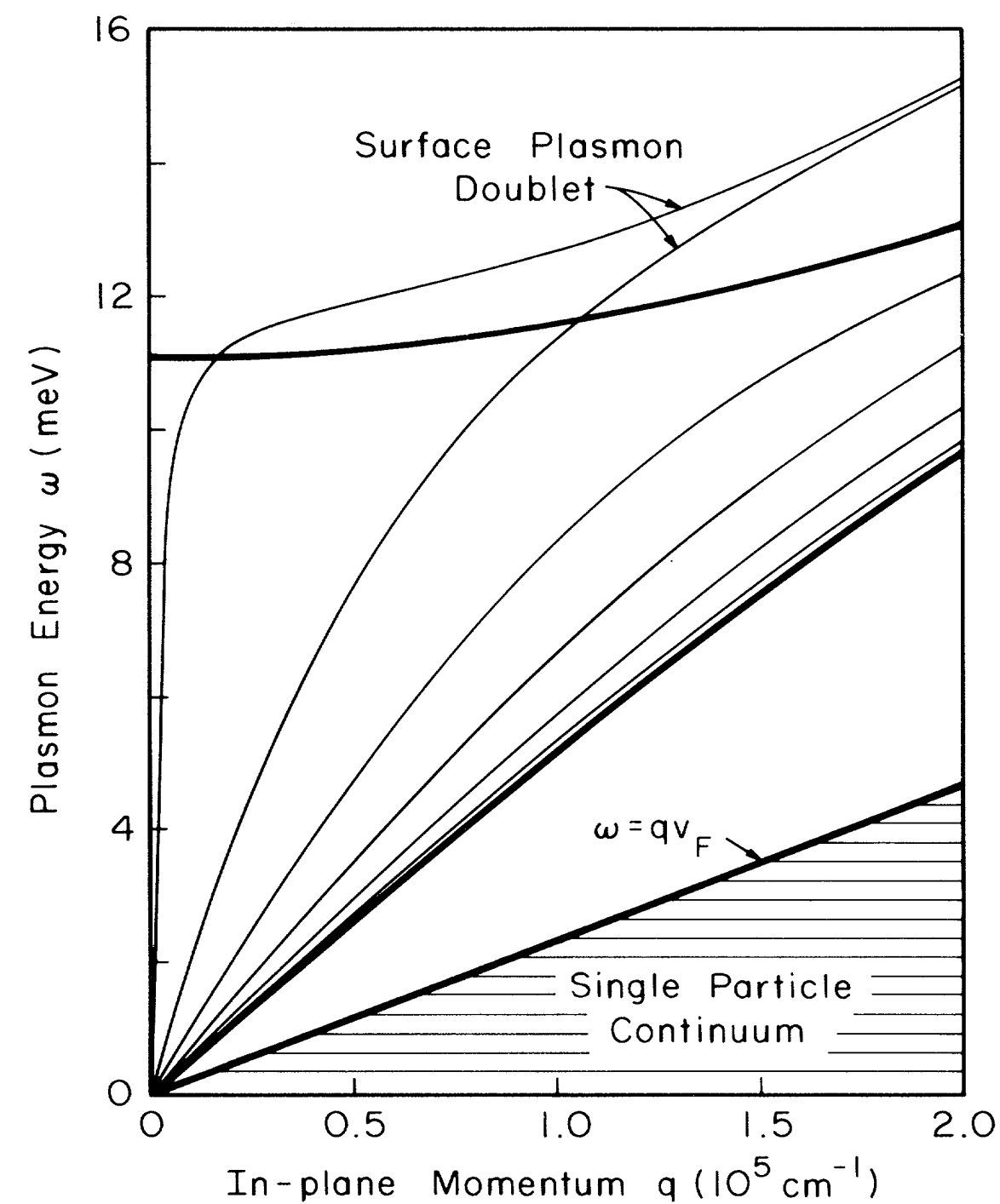


FIG. 1. Collective modes (thin lines) of a film containing six 2DEG layers. The boundaries of the bulk plasmon band (thick lines) and the single-particle continuum are also shown.

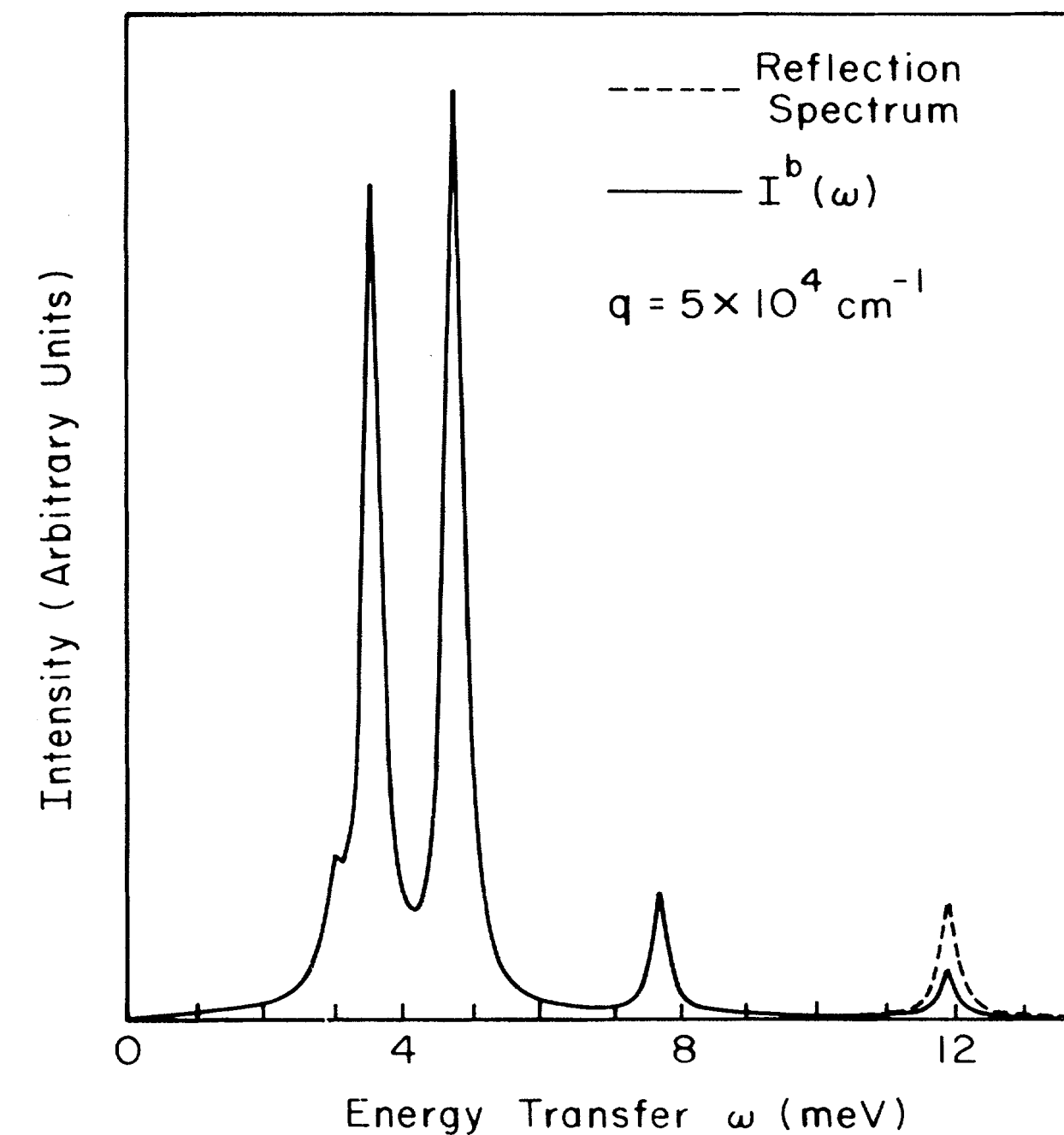


FIG. 4. The solid line is the intensity of the backscattered light,  $I^b(\omega)$ . The intensity is plotted on the same scale as in Fig. 3. The peaks at 3.5 and 4.5 meV appear most strongly. These are the modes that lie close to the bulk plasmon energy  $\sim 4$  meV. The total reflected Raman intensity differs from  $I^b$  only at the dashed line.

## Discrete Plasmons in Finite Semiconductor Multilayers

A. Pinczuk, M. G. Lamont, and A. C. Gossard  
*AT&T Bell Laboratories, Murray Hill, New Jersey 07974*  
 (Received 19 November 1985)

We observe discrete plasmons in layered 2D electron gases with a large, but finite, number of periods. The twofold degeneracy of plasmon modes with wave numbers in the first Brillouin zone of the infinite system is lifted by the loss of complete periodicity in the finite system. These characteristic discrete plasmon doublets are measured in inelastic-light-scattering spectra of multilayer GaAs/(AlGa)As heterostructures.

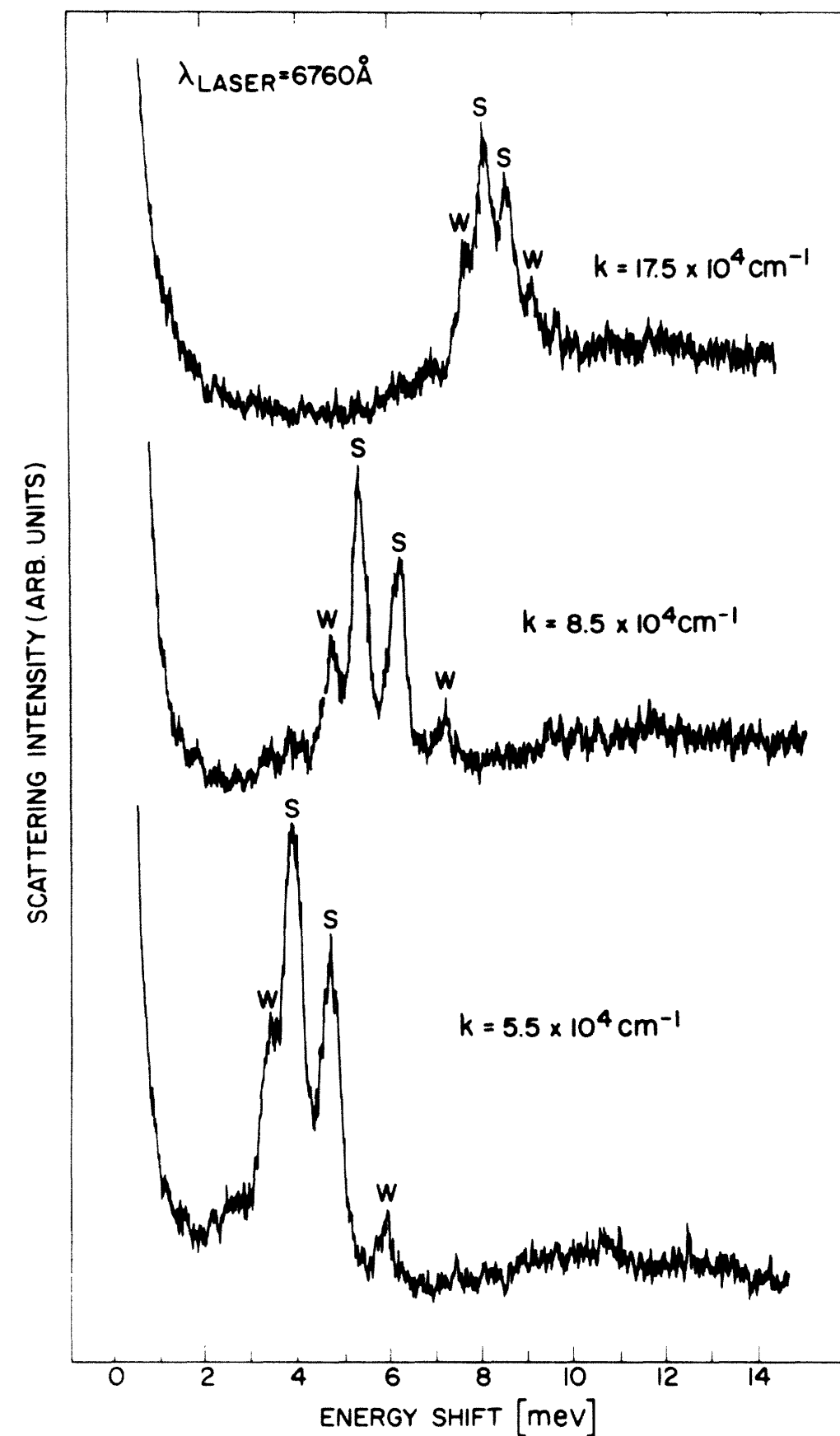


FIG. 1. Inelastic-light-scattering spectra of discrete plasmons taken at different values of the in-plane scattering wave vector  $k$ . The spectra were excited with a laser wavelength of  $\lambda_L = 6760 \text{ \AA}$ .

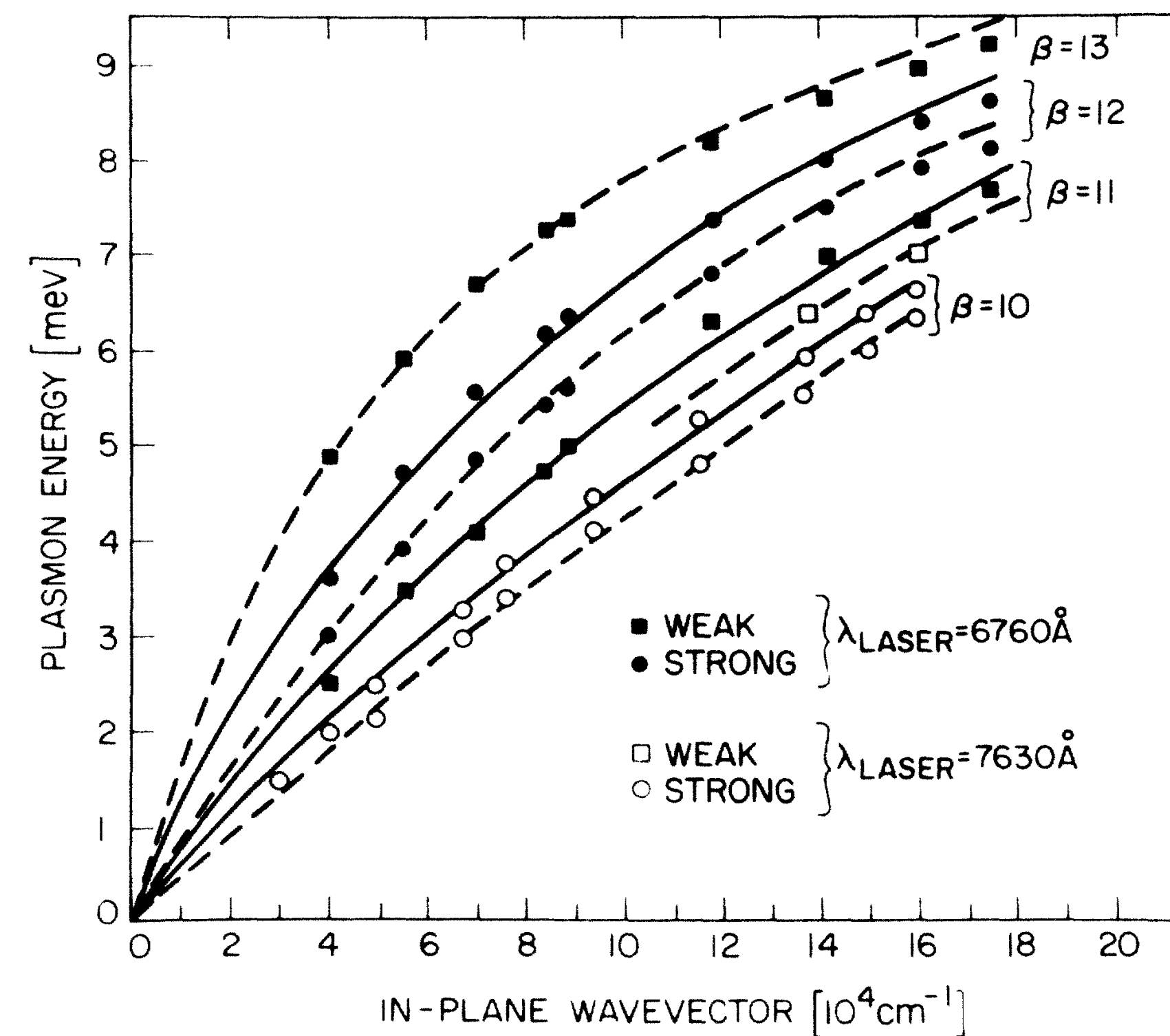
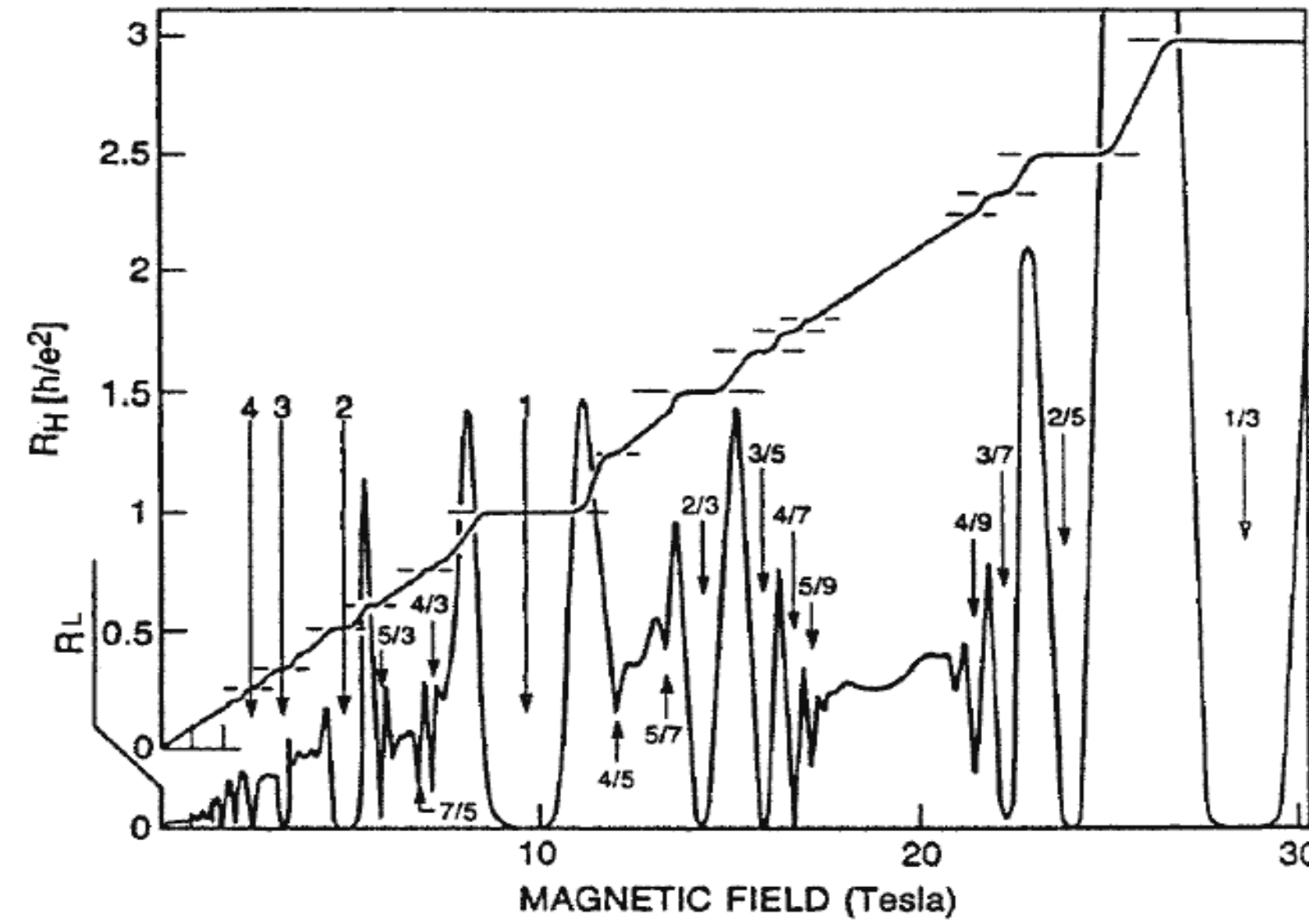


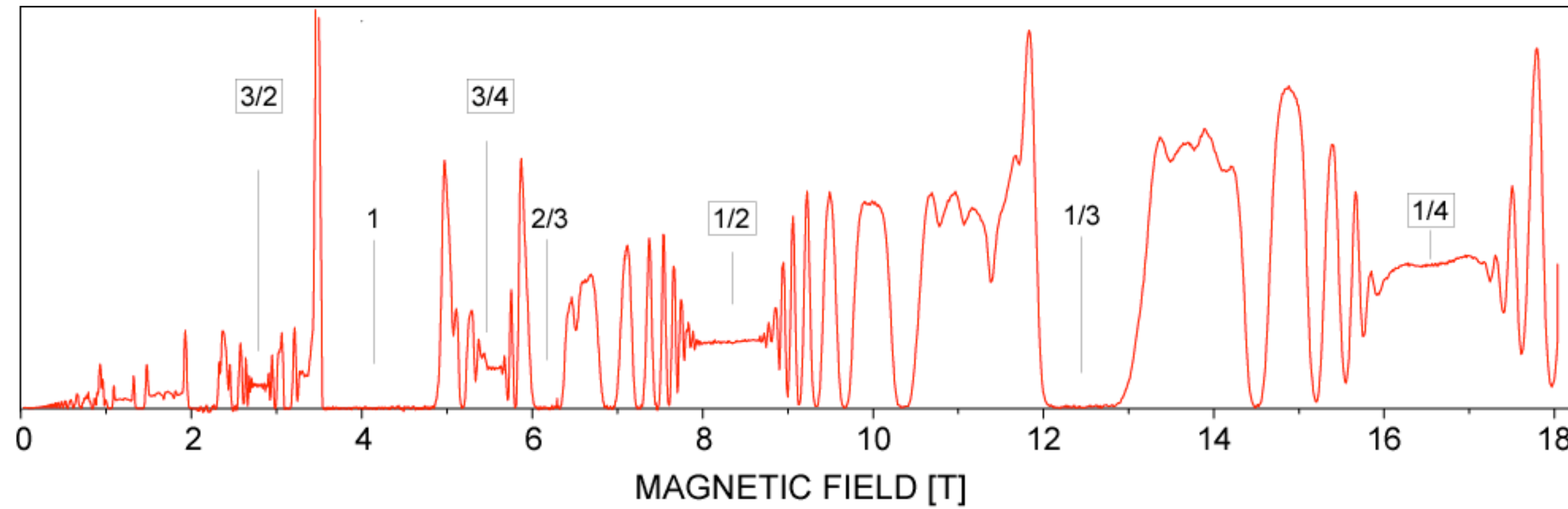
FIG. 3. The points are the peak positions in light-scattering spectra of discrete plasmons plotted as a function of the in-plane scattering wave vectors. The lines are the calculated discrete plasmon dispersions.

**FQHE**

$$R_H = \frac{h}{fe^2}$$



Willett et al.



Pan, Pfeiffer, Stormer, et al.

- The FHQE state is one of the most amazing collective states of matter.

# **Neutral modes in FQHE: SMA**

### Collective-Excitation Gap in the Fractional Quantum Hall Effect

S. M. Girvin

*Surface Science Division, National Bureau of Standards, Gaithersburg, Maryland 20899*

and

A. H. MacDonald

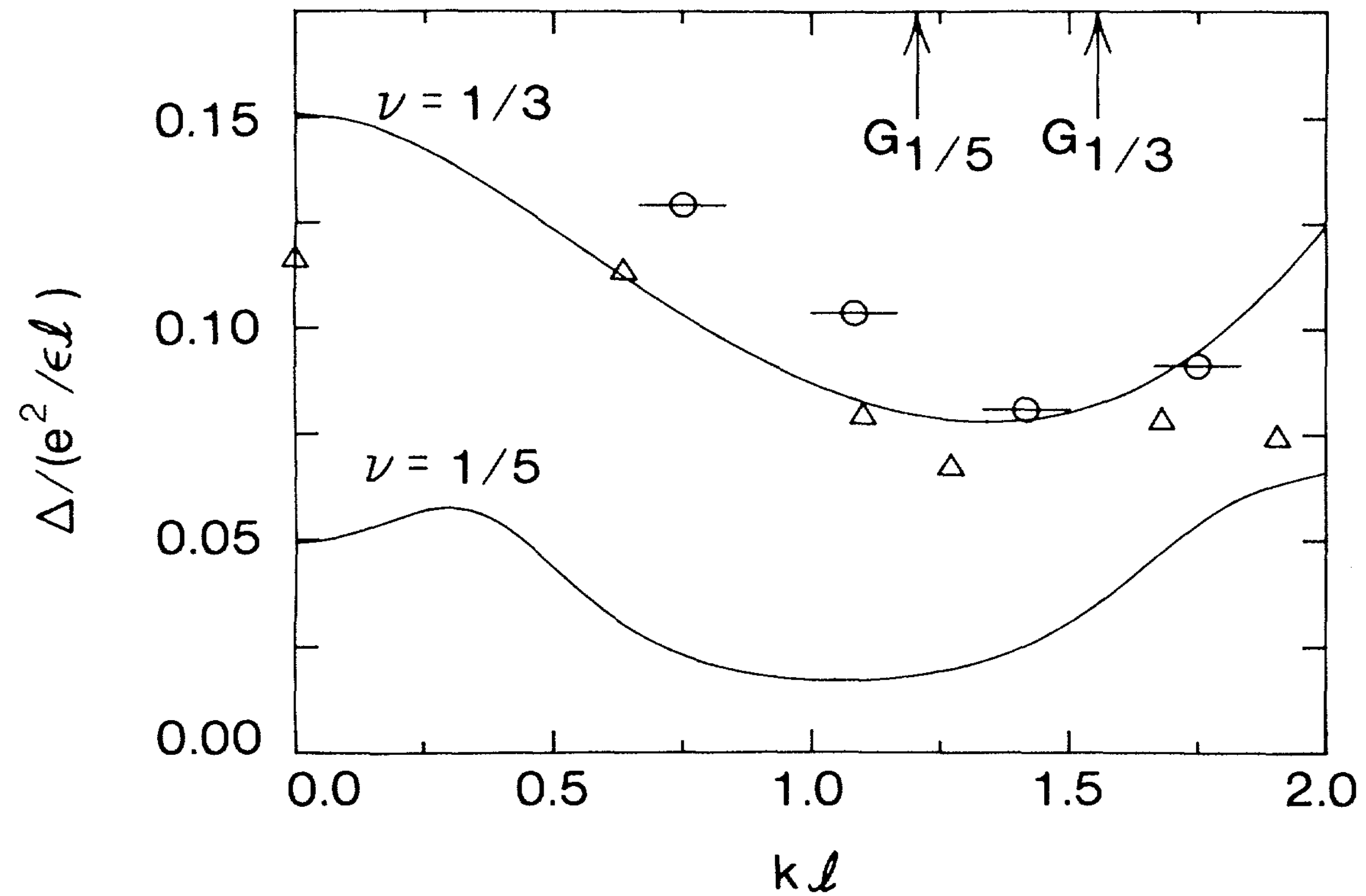
*National Research Council of Canada, Ottawa, K1A 0R6, Canada*

and

P. M. Platzman

*AT&T Bell Laboratories, Murray Hill, New Jersey 07974*

(Received 25 October 1984)



**Single mode approximation**

$$\Psi_{\mathbf{k}} = P_{LLL} \rho_{\mathbf{k}} \Psi_{GS}$$

## Observation of Collective Excitations in the Fractional Quantum Hall Effect

A. Pinczuk, B. S. Dennis, L. N. Pfeiffer, and K. West  
*AT&T Bell Laboratories, Murray Hill, New Jersey 07974*  
 (Received 27 January 1993)

Kang, Pinczuk et al. *PRL* 86, 2637 (2001)  
 Energy (meV)

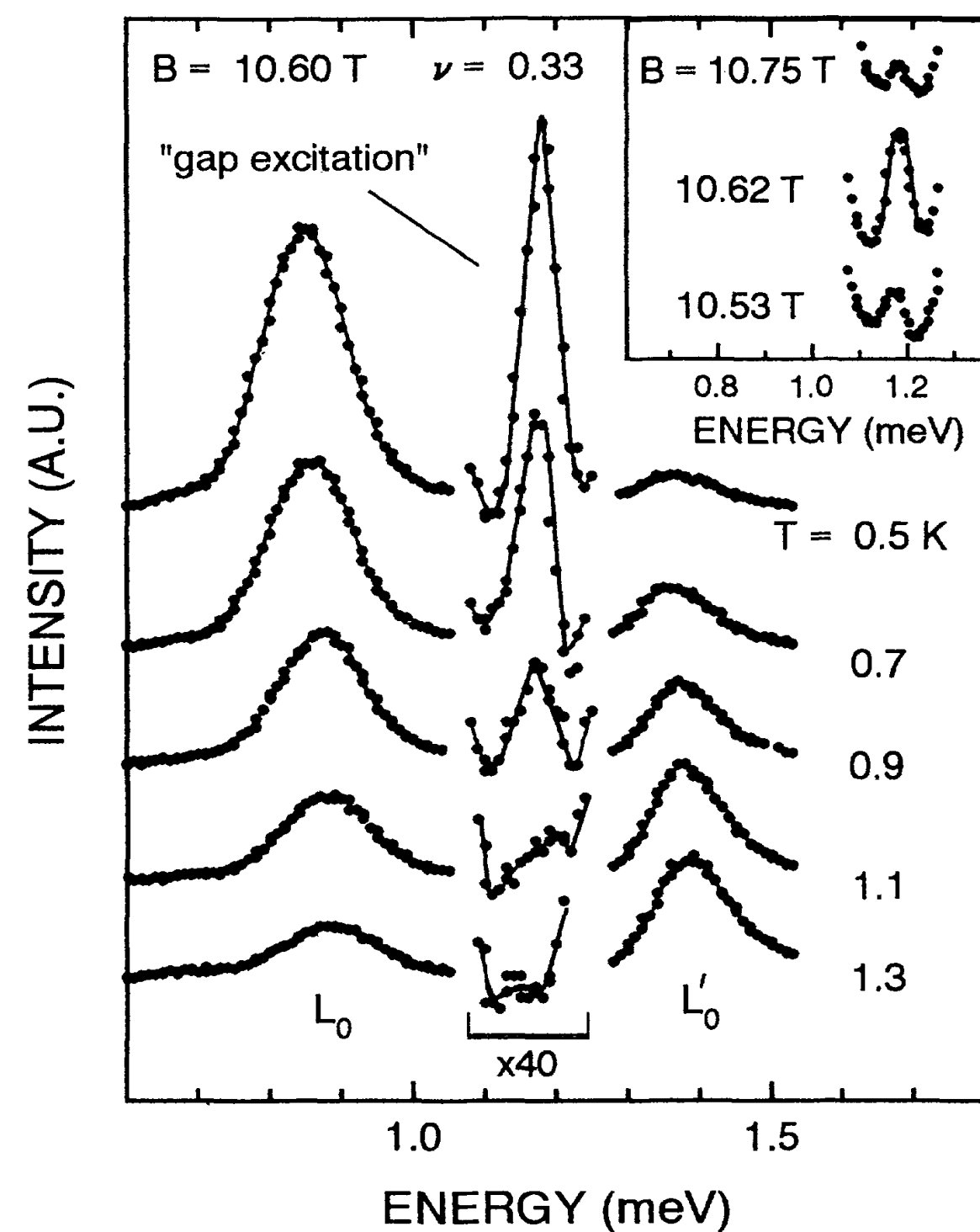


FIG. 1. Temperature dependence of inelastic light scattering spectra of a low-lying excitation of the FQHE at  $\nu = \frac{1}{3}$ . The single quantum well has density  $n = 8.5 \times 10^{10} \text{ cm}^{-2}$ . The inset shows the  $B$  dependence of the 0.5 K spectra. The light scattering peak, labeled “gap excitation,” is interpreted as a  $q = 0$  collective gap excitation. The bands labeled  $L_0$  and  $L'_0$  comprise the characteristic doublets of intrinsic photoluminescence. The temperature dependence of the  $L_0$  and  $L'_0$  intensities is due to the optical anomaly at  $\nu = \frac{1}{3}$ .

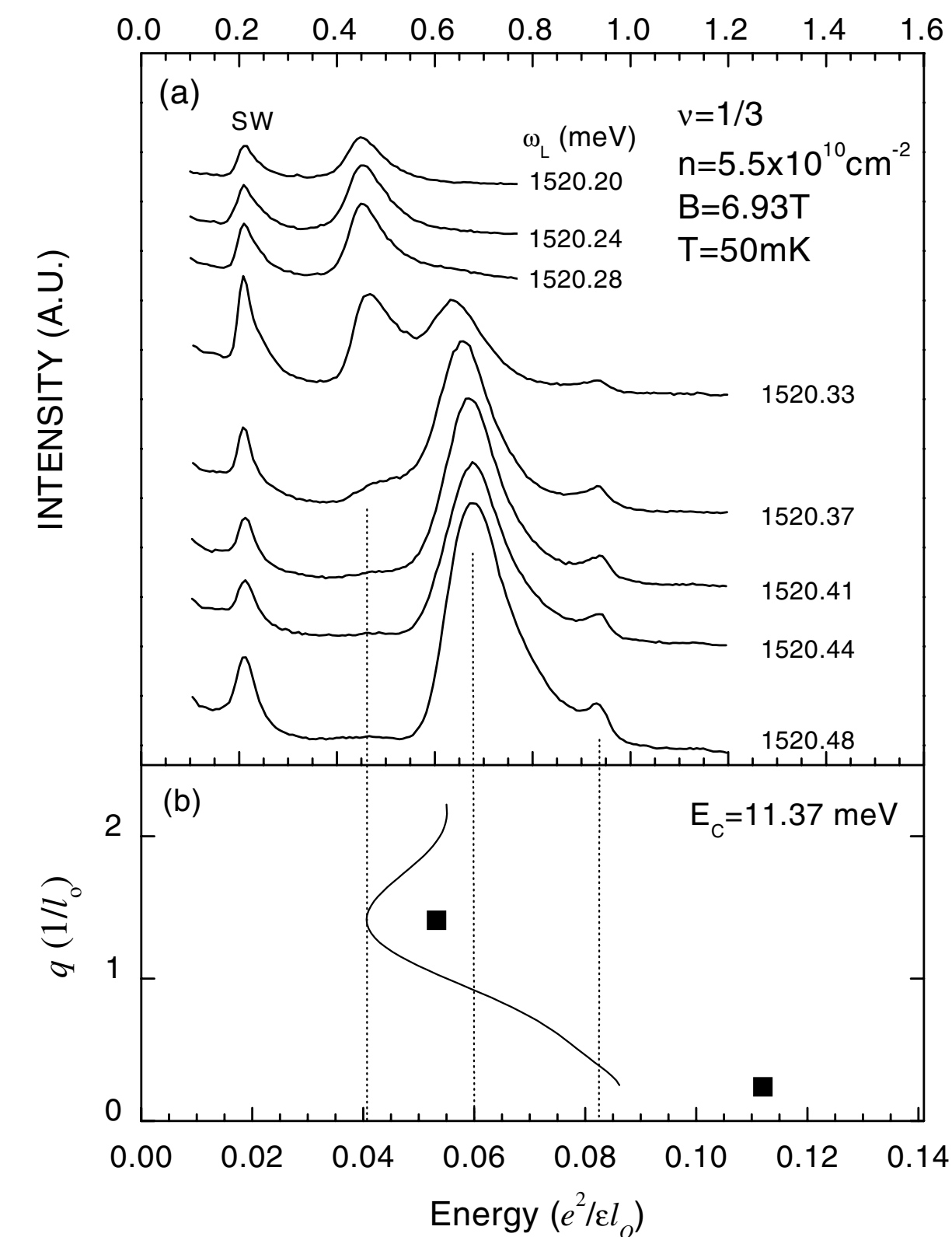


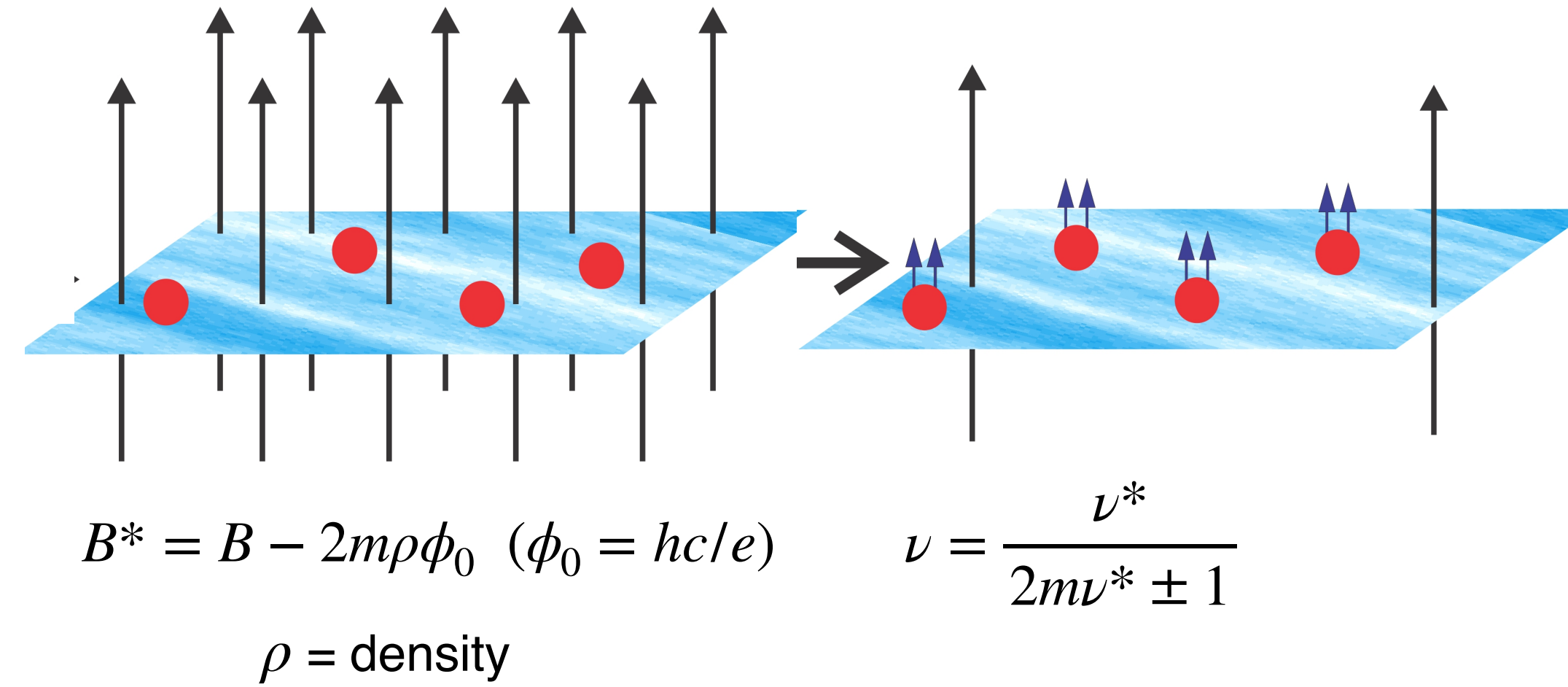
FIG. 1. (a) Resonant inelastic light scattering spectra at  $\nu = \frac{1}{3}$ . SW denotes the long wavelength spin wave excitation at the Zeeman energy  $E_Z = g\mu_B B_T$ , where  $g = 0.43 \pm 0.01$ . Dotted lines indicate collective excitations of the FQH state. (b) The dispersion of collective excitations at  $\nu = \frac{1}{3}$ . The solid curve was scaled down from the ideal 2D result [10] by a constant to help in assigning the observed modes. Solid squares indicate results of calculations that incorporate the effect of finite thickness [24].

- Light scattering can also reveal finite wave vector roton minima due to disorder.

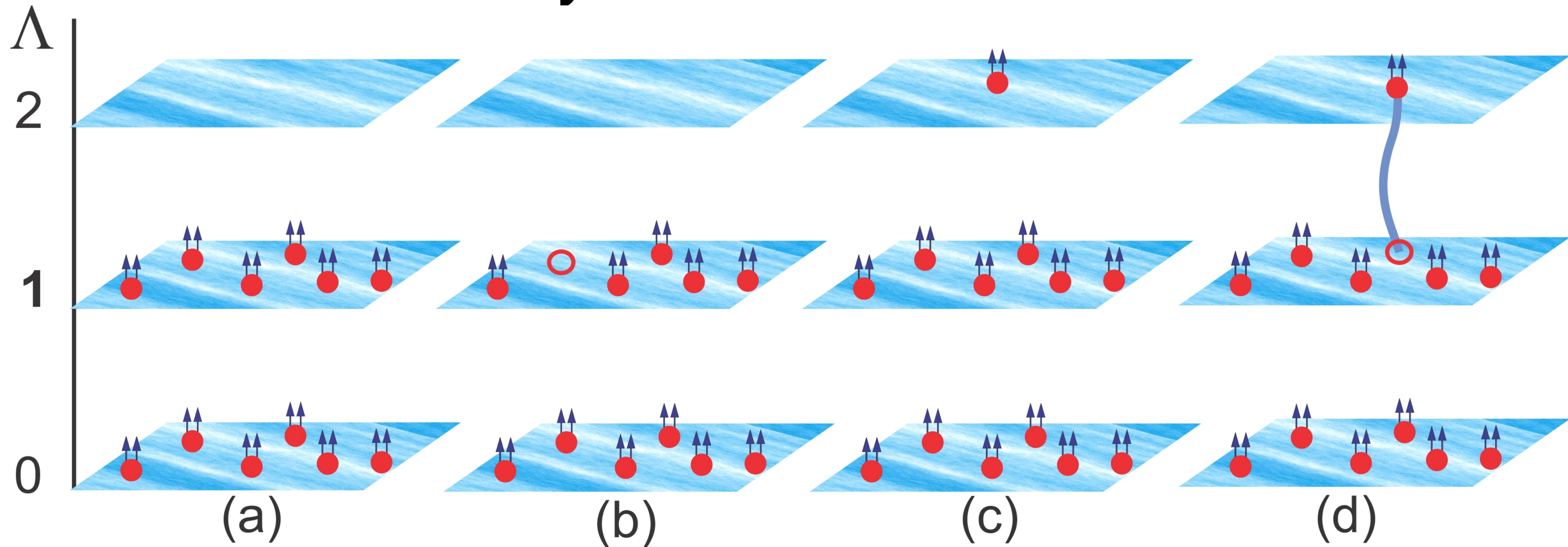
# **Neutral modes in FQHE: CF excitons**

# Composite fermions

Strongly interacting electrons at  $B = \nu$  = weakly interacting composite fermions at  $B^* = B - 2m\rho\phi_0$



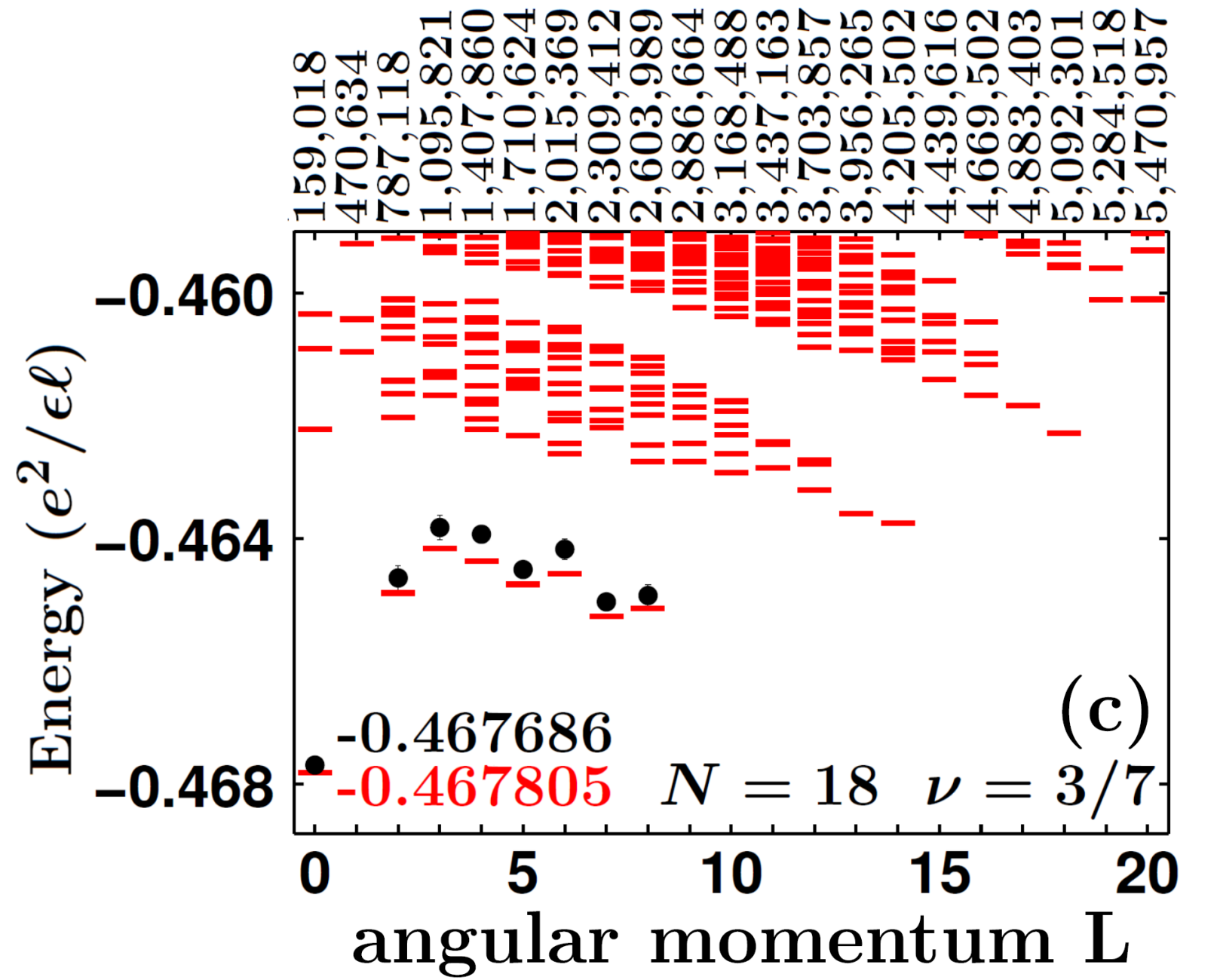
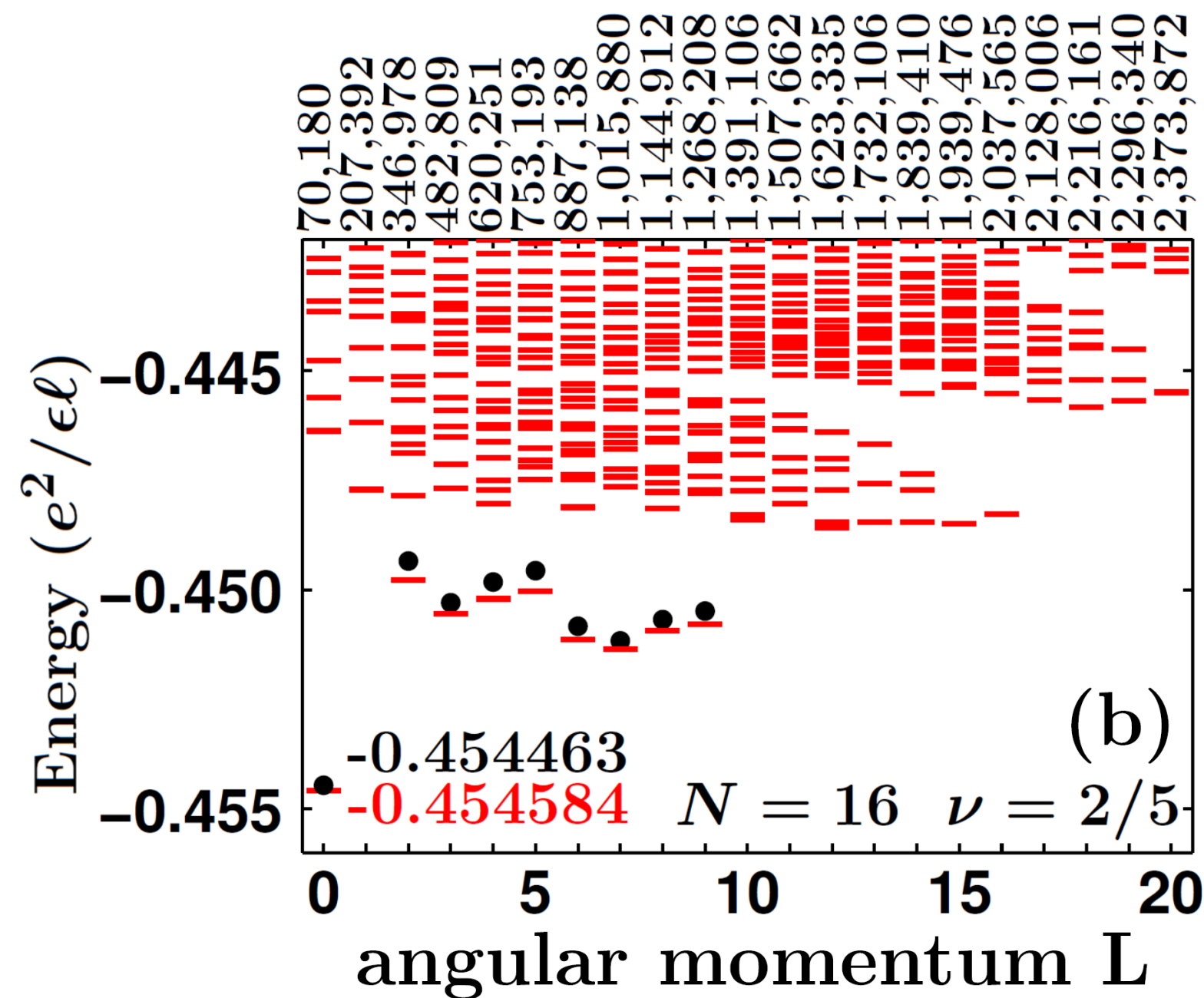
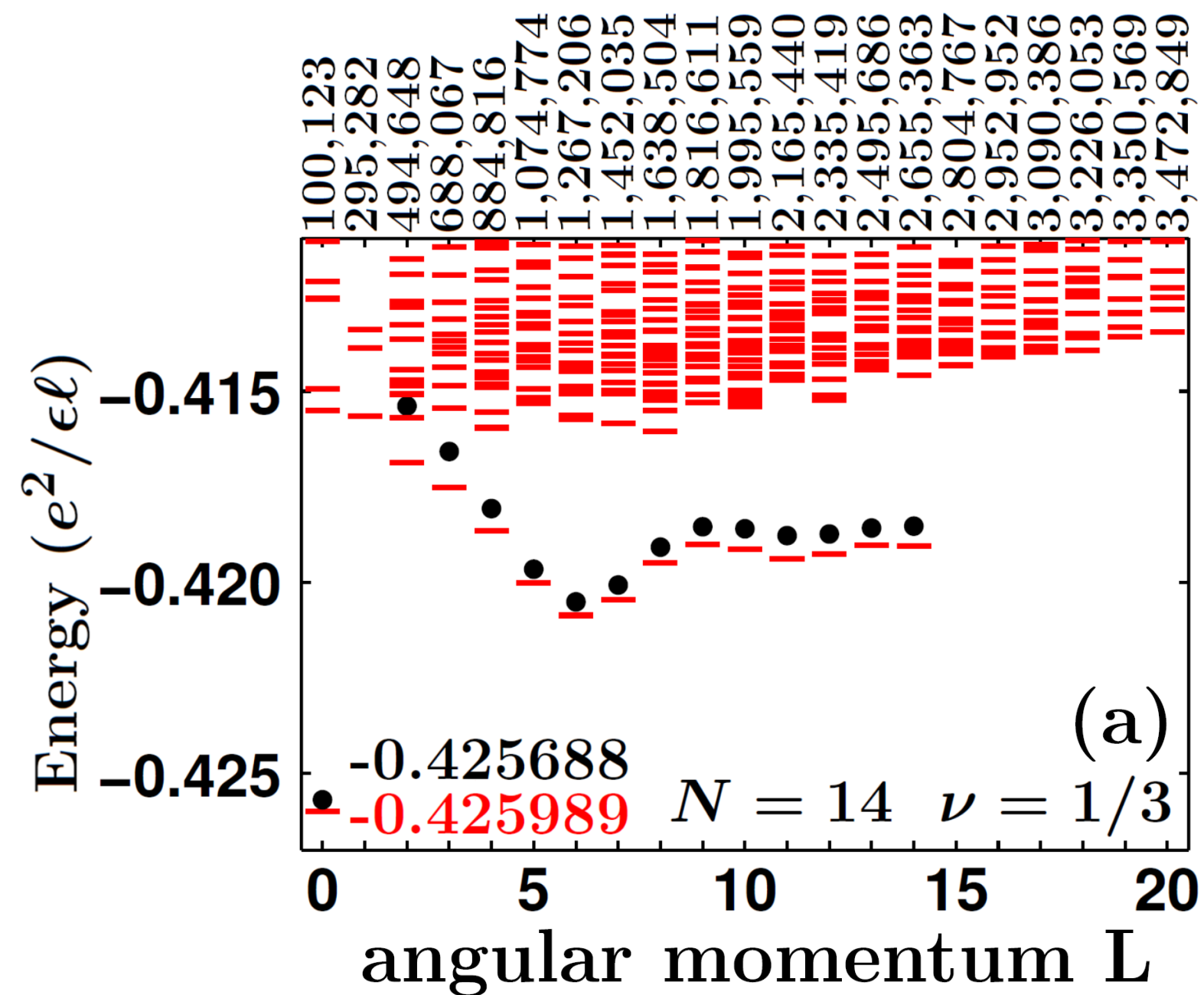
# CF theory of neutral excitations



- The ground state at  $\nu = n/(2n + 1)$  is  $\nu^* = n$  filled levels of composite fermions; its quasihole is a missing CF; quasiparticle is an isolated CF; and neutral excitations are CF-particle hole pairs. The wave functions of these are obtained from the known wave functions at integer fillings by composite-fermionization.
- Question: How well does the CF theory work? What all can it explain?

$$\Psi_{\frac{n}{2n+1}} = P_{\text{LLL}} \Phi_n \prod_{j < k} (z_j - z_k)^2$$

# Comparison with exact diagonalization studies



- The CF exciton theory obtains the dispersions of the neutral excitations at all  $\nu = n/(2pn \pm 1)$  fractions qualitatively and quantitatively.

## Rotons of composite fermions: Comparison between theory and experiment

Vito W. Scarola, Kwon Park, and Jainendra K. Jain

Department of Physics, 104 Davey Laboratory, The Pennsylvania State University, University Park, Pennsylvania 16802

(Received 27 December 1999)

**The CF excitons at  $\nu = n/(2n \pm 1)$  have  $n$  primary roton minima.**

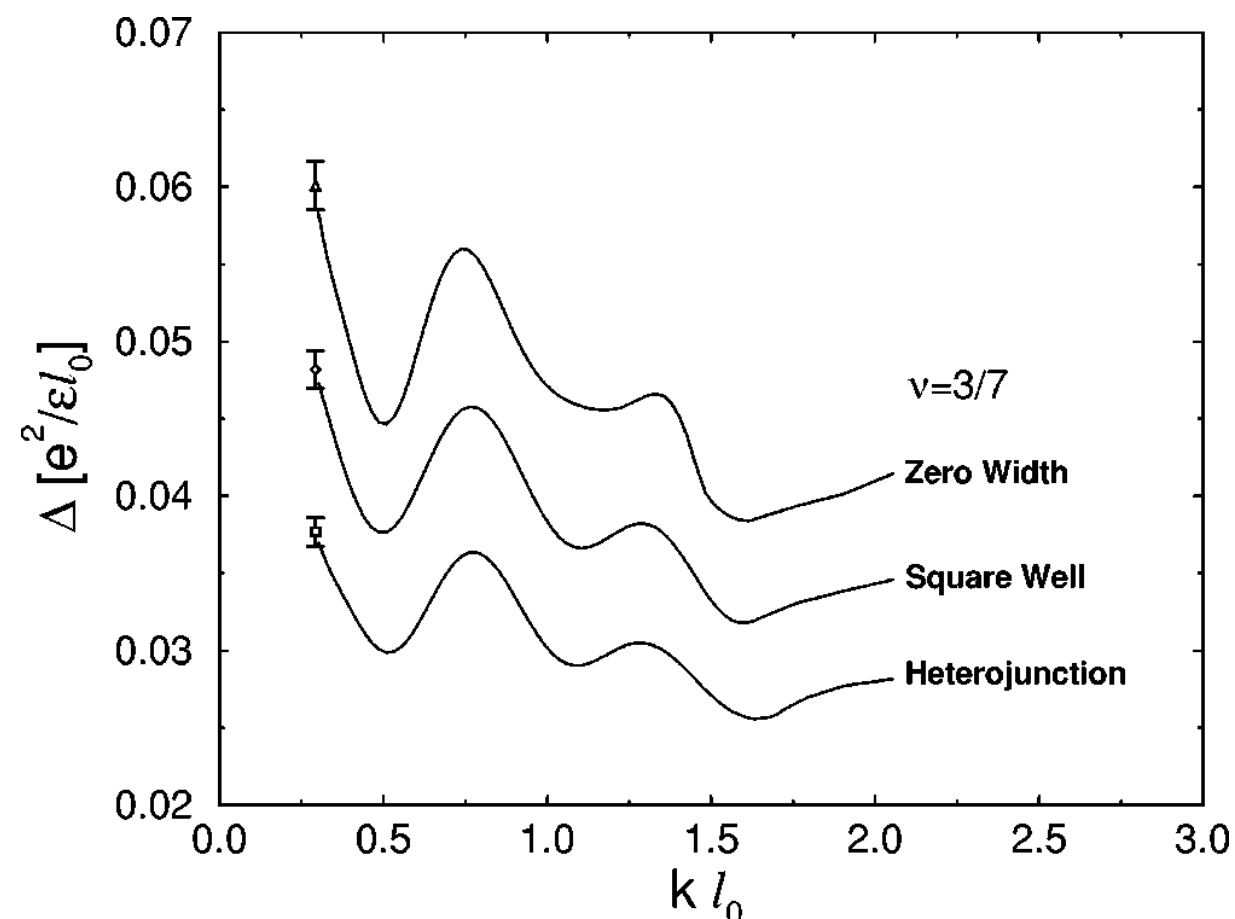
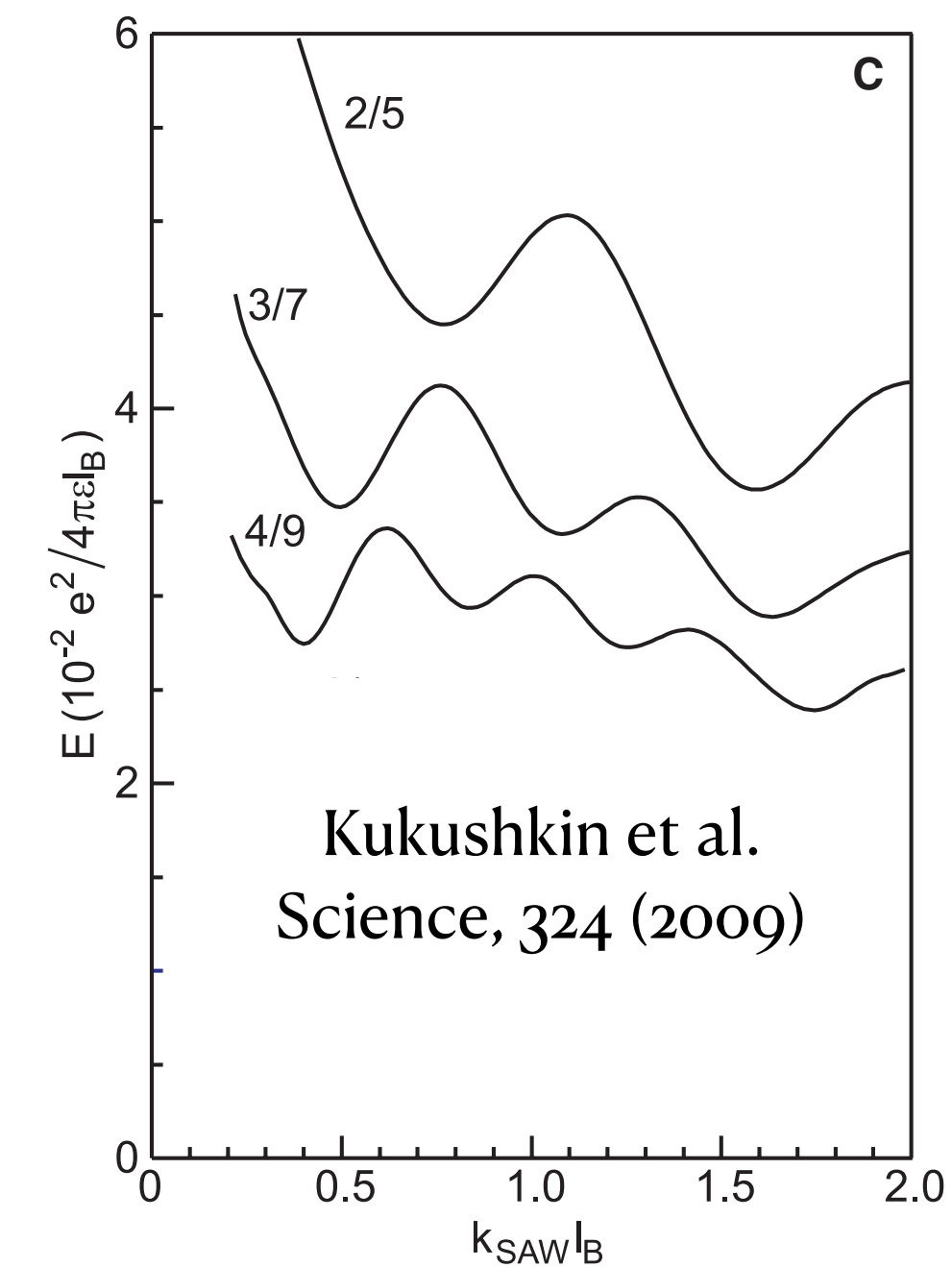


FIG. 2. The dispersions of the CF exciton at  $\nu=3/7$  for a zero width system, for a heterojunction (with density  $1.5 \times 10^{11} \text{ cm}^{-2}$ ), and for a square quantum well of width 30 nm (with density  $0.5 \times 10^{11} \text{ cm}^{-2}$ ). The dispersions are for a system of 63 composite fermions, obtained by interpolation through the discrete  $k$  values available in the study.

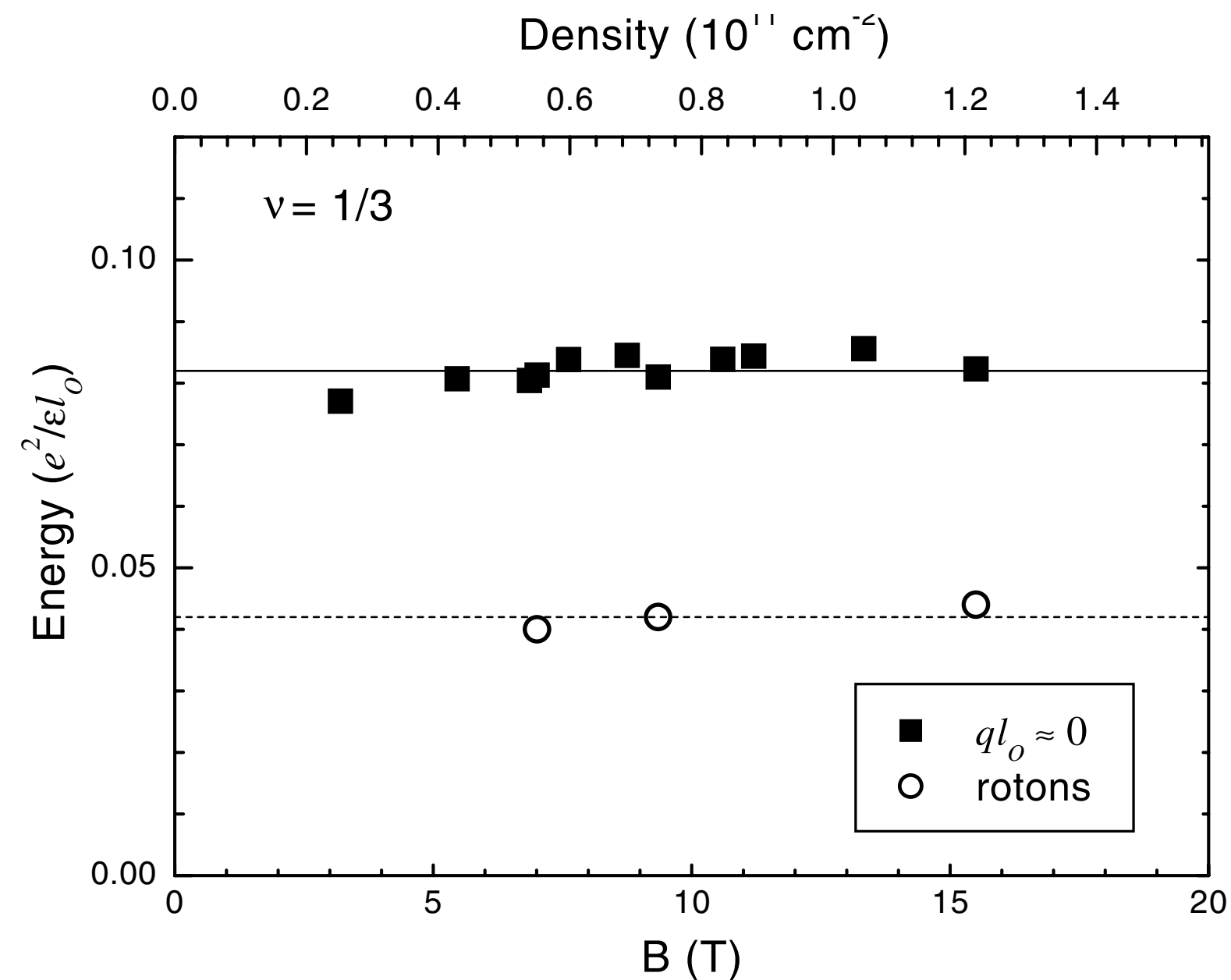


FIG. 3. Collective gap excitations at  $\nu = 1/3$  from samples with various densities ( $n$ ) within  $2.4 \times 10^{10} \leq n \leq 1.2 \times 10^{11} \text{ cm}^{-2}$ . Collective gap excitation energies are measured in terms of the Coulomb energy,  $E_C = e^2/\epsilon l_0$ .

**Kang, Pinczuk et al. PRL 86, 2637 (2001)**

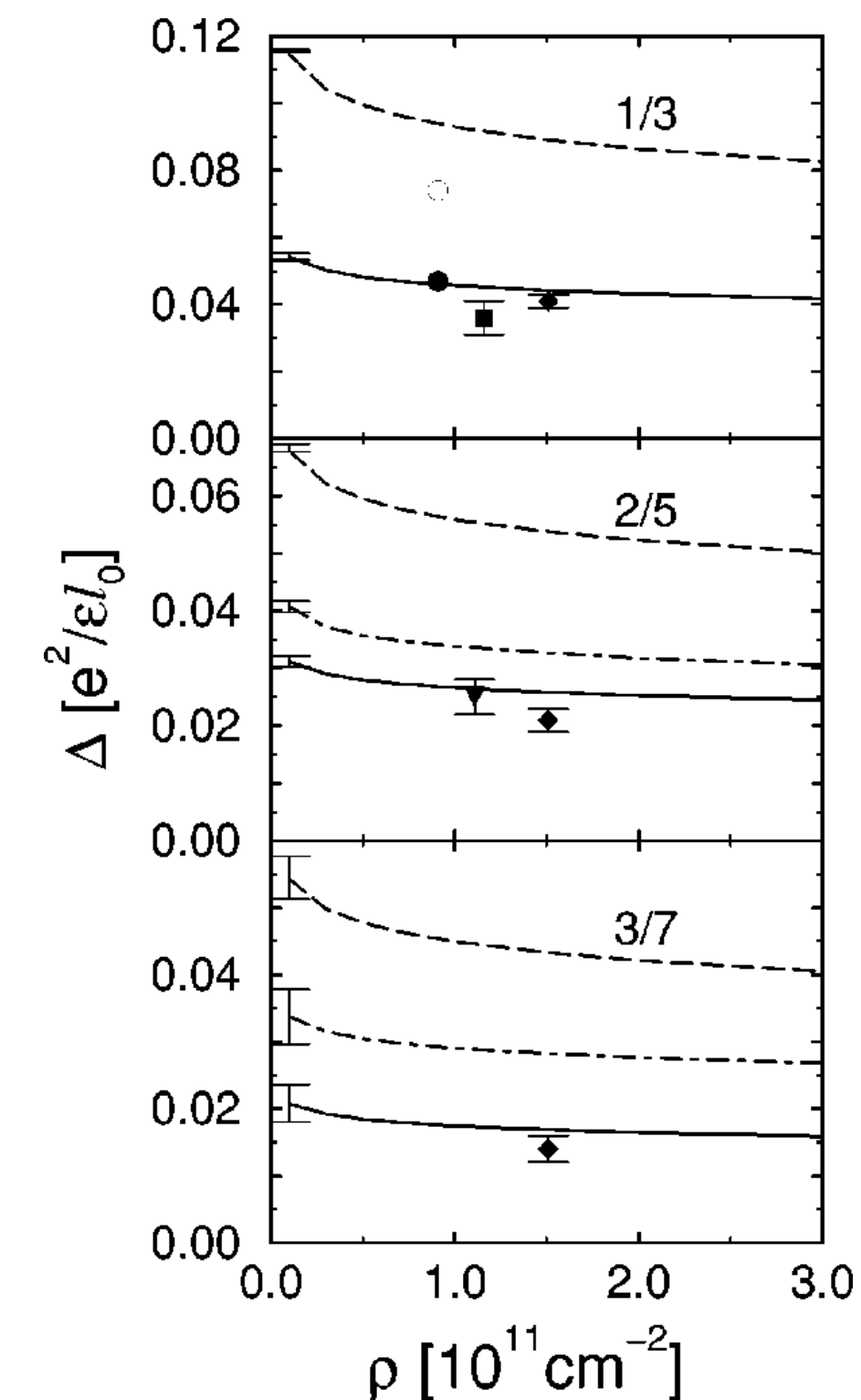


FIG. 5. The energies of the fundamental and the secondary rotors (solid and dash-dotted lines, respectively) and of the CF exciton in the long-wavelength limit (dashed line) as a function of the density for a heterojunction. Experimental energies are also shown, taken from Refs. 8 (circle), 9 (diamond), 10 (square), and 11 (down-triangle); the filled symbols correspond to the roton, and the empty ones to the long-wavelength mode.

## Observation of Multiple Magnetorotons in the Fractional Quantum Hall Effect

Moonsoo Kang,<sup>1,2,\*</sup> A. Pinczuk,<sup>1,2</sup> B. S. Dennis,<sup>2</sup> L. N. Pfeiffer,<sup>2</sup> and K. W. West<sup>2</sup>

<sup>1</sup>Departments of Applied Physics and Physics, Columbia University, New York, New York 10027

<sup>2</sup>Bell Labs, Lucent Technologies, Murray Hill, New Jersey 07974

(Received 5 October 2000)

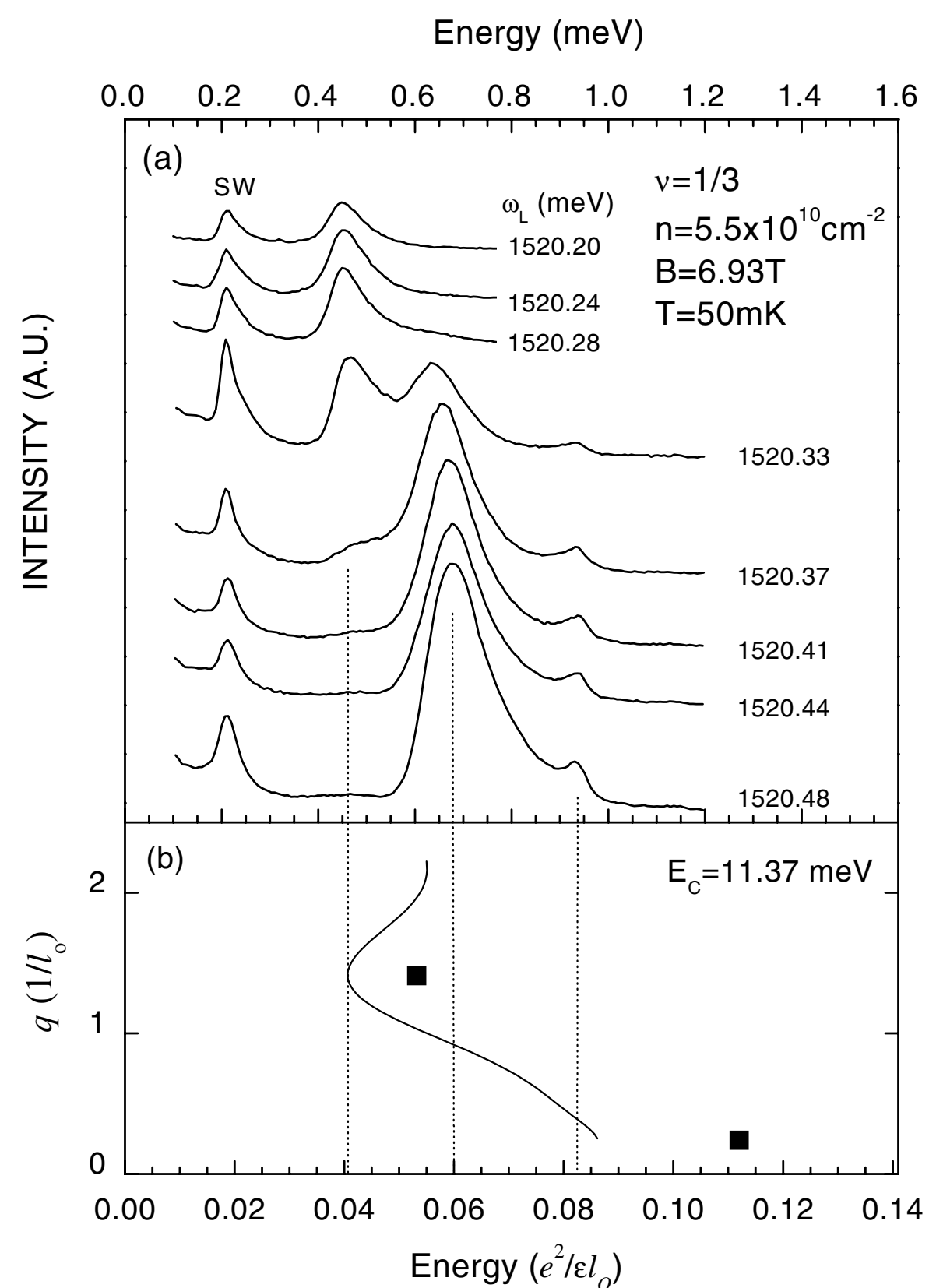


FIG. 1. (a) Resonant inelastic light scattering spectra at  $\nu = 1/3$ . SW denotes the long wavelength spin wave excitation at the Zeeman energy  $E_Z = g\mu_B B_T$ , where  $g = 0.43 \pm 0.01$ . Dotted lines indicate collective excitations of the FQH state. (b) The dispersion of collective excitations at  $\nu = 1/3$ . The solid curve was scaled down from the ideal 2D result [10] by a constant to help in assigning the observed modes. Solid squares indicate results of calculations that incorporate the effect of finite thickness [24].

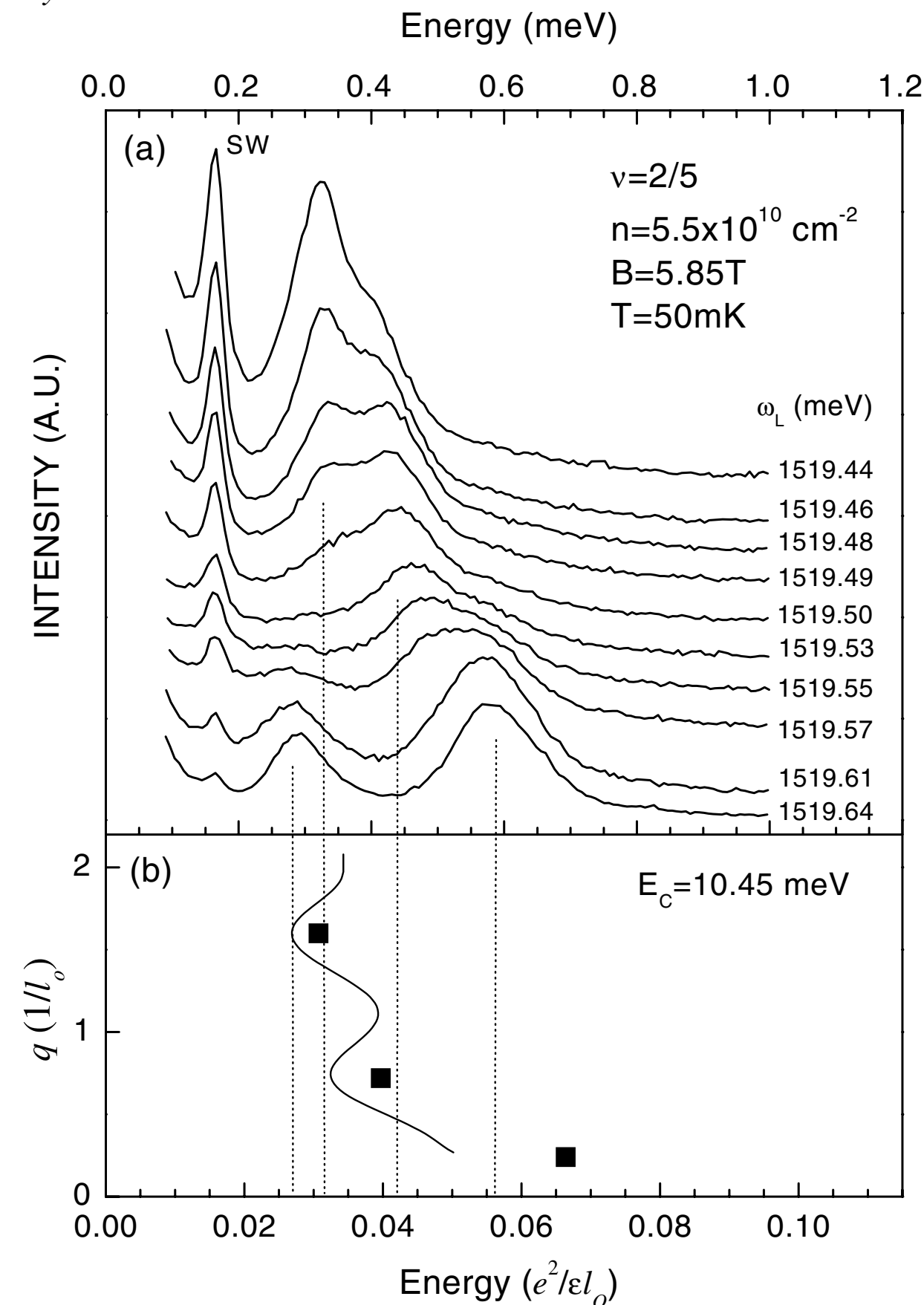


FIG. 2. (a) Resonant inelastic light scattering spectra at  $\nu = 2/5$ . Dotted lines denote collective excitations in the FQH state. (b) The dispersion of collective excitations at  $\nu = 2/5$ . The solid curve was scaled down from the ideal 2D result [10] by a constant, as in Fig. 1(b). Solid squares indicate results of calculations that incorporate the effect of finite thickness [24].

**High energy neutral modes**

## Splitting of Long-Wavelength Modes of the Fractional Quantum Hall Liquid at $\nu = 1/3$

C. F. Hirjibehedin,<sup>1,2,\*</sup> Irene Dujovne,<sup>3,2</sup> A. Pinczuk,<sup>1,2,3</sup> B. S. Dennis,<sup>2</sup> L. N. Pfeiffer,<sup>2</sup> and K. W. West<sup>2</sup>

<sup>1</sup>Department of Physics, Columbia University, New York, New York 10027, USA

<sup>2</sup>Bell Labs, Lucent Technologies, Murray Hill, New Jersey 07974, USA

<sup>3</sup>Department of Applied Physics and Applied Mathematics, Columbia University, New York, New York 10027, USA

(Received 17 February 2004; published 2 August 2005)

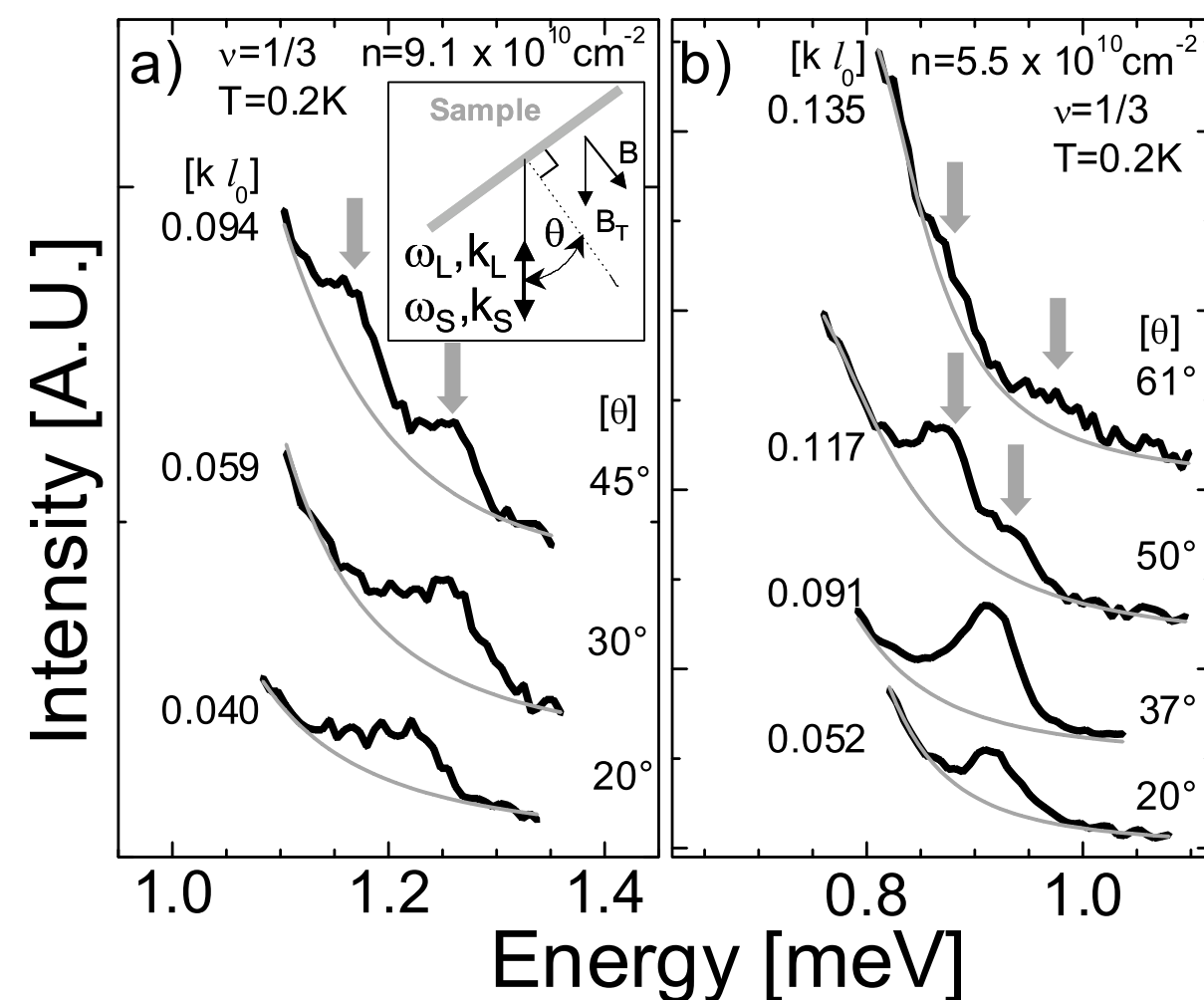


FIG. 1. Inelastic light scattering spectra of low-lying long-wavelength charge modes at  $\nu = 1/3$  at various angles  $\theta$  in (a) sample A and (b) sample B. The spectra are also labeled by the equivalent wave vector  $k = (2\omega_L/c)\sin\theta$  in units of  $1/l_0$ . The gray arrows highlight the splitting of the single peak at small wave vectors into two peaks at larger wave vectors. The light gray lines show the background. The upper inset in panel (a) shows the inelastic light scattering geometry.

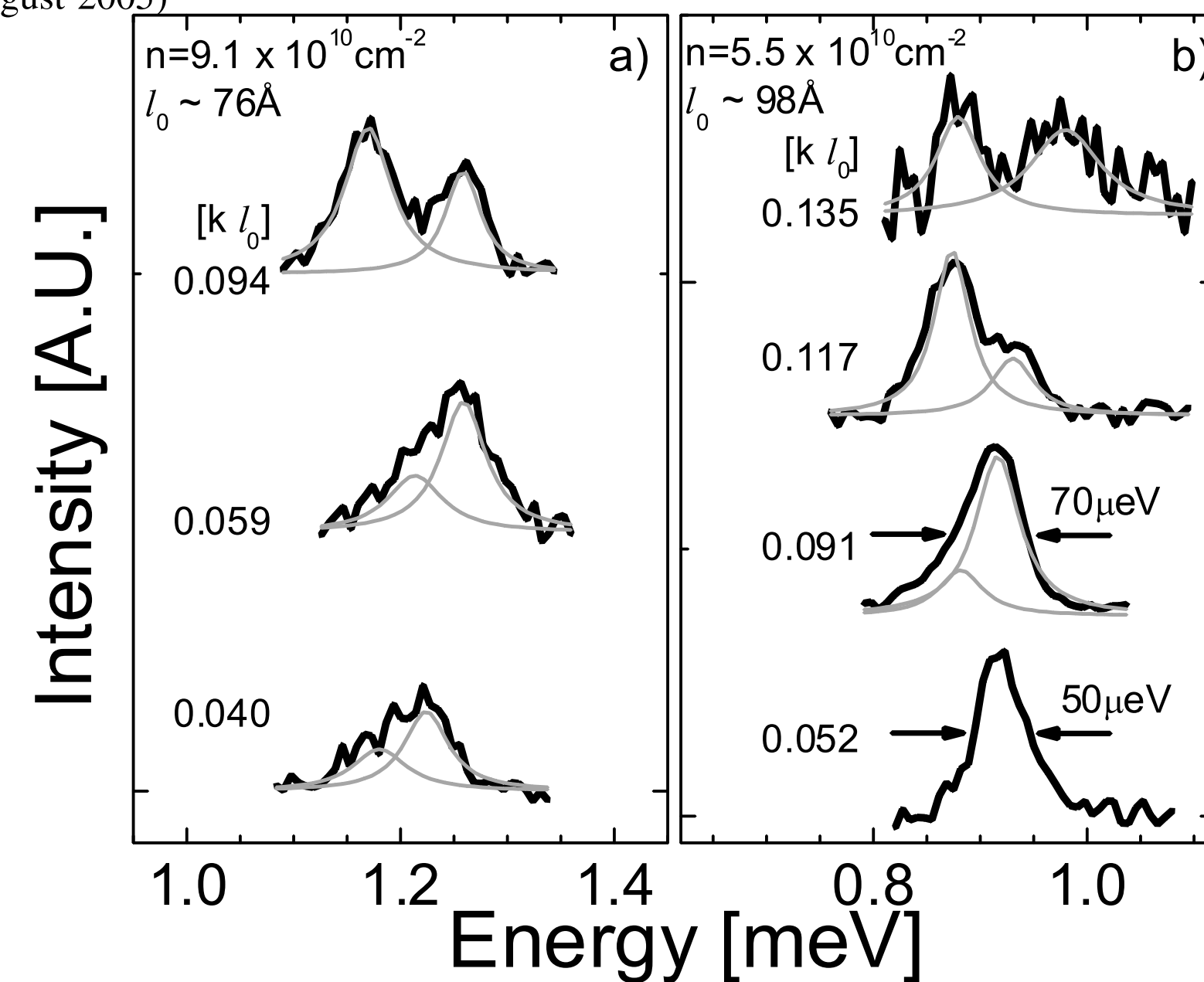
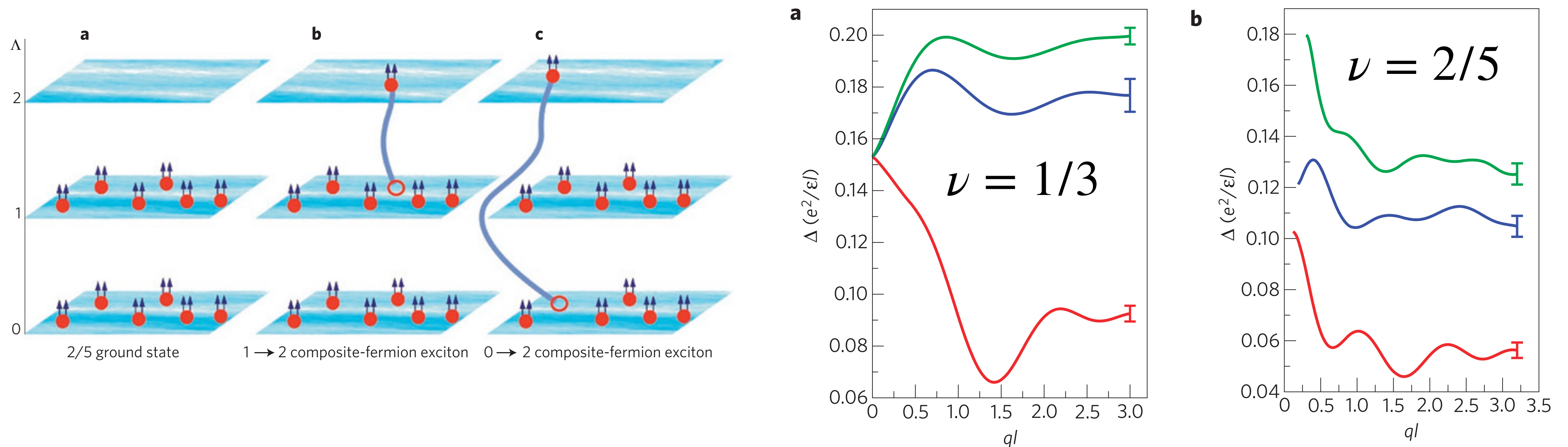


FIG. 2. Spectra from Figs. 1(a) and 1(b) with backgrounds subtracted. The gray lines show fits with two Lorentzian line shapes.

- The  $q = 0$  mode at  $\nu = 1/3$  splits into a doublet at finite  $q$  !

# Collective excitations of composite fermions across multiple $\Lambda$ levels

Dwipesh Majumder<sup>1</sup>, Sudhansu S. Mandal<sup>1</sup> and Jainendra K. Jain<sup>2\*</sup>



- Surprisingly, the energies of CF excitons across multiple CF Landau levels merge at  $q = 0$  at  $\nu = 1/3$ .
- Theoretical splitting of  $0.013(5)e^2/\epsilon l$  at  $ql = 0.15$  is in good agreement with experiment ( $\sim 0.012(3)$ ).
- The splitting seen in experiments thus represents a CF exciton across two CF Landau levels.

## Higher-Energy Composite Fermion Levels in the Fractional Quantum Hall Effect

Trevor D. Rhone,<sup>1</sup> Dwipesh Majumder,<sup>2</sup> Brian S. Dennis,<sup>3</sup> Cyrus Hirjibehedin,<sup>4</sup> Irene Dujovne,<sup>5</sup> Javier G. Groshaus,<sup>6</sup> Yann Gallais,<sup>7</sup> Jainendra K. Jain,<sup>8</sup> Sudhansu S. Mandal,<sup>2</sup> Aron Pinczuk,<sup>1,5</sup> Loren Pfeiffer,<sup>9</sup> and Ken West<sup>9</sup>

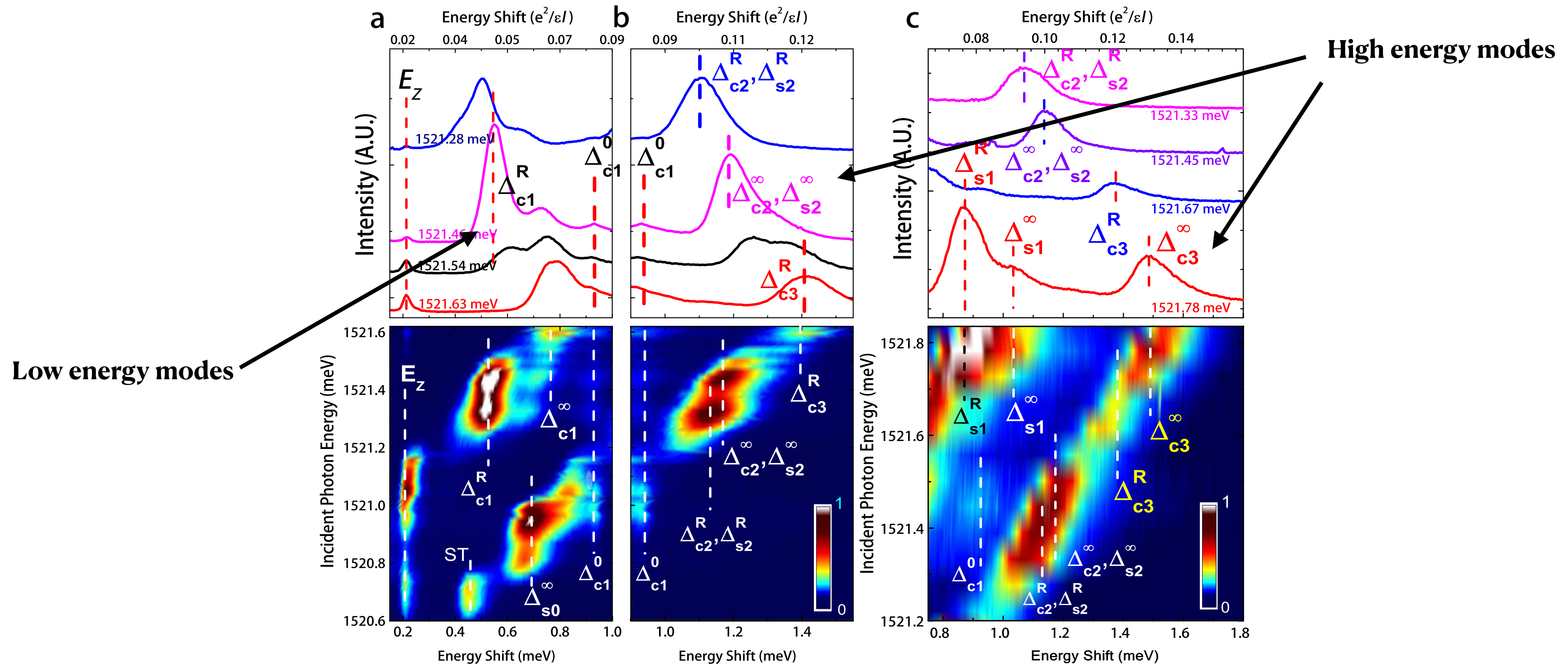


FIG. 2 (color online). ILS spectra of excitations at  $\nu = 1/3$  as a function of the energy shift (with total magnetic field  $B_T = 8.0$  T, and a tilt of  $30^\circ$ ). The energy is shown in units of  $e^2/\epsilon l$  on the top scale, where  $l$  is magnetic length and  $\epsilon$ , the dielectric constant of GaAs. The upper panels show peaks of several modes for certain selected incident photon energies. The lower panel contains a color plot of the intensities of both (a) “low energy” and (b),(c) the novel high-energy modes. The vertical lines mark the positions of the collective modes. The symbols, explained in the text, identify the modes with excitations of CFs across several  $\Lambda$  levels, both with and without spin reversal.

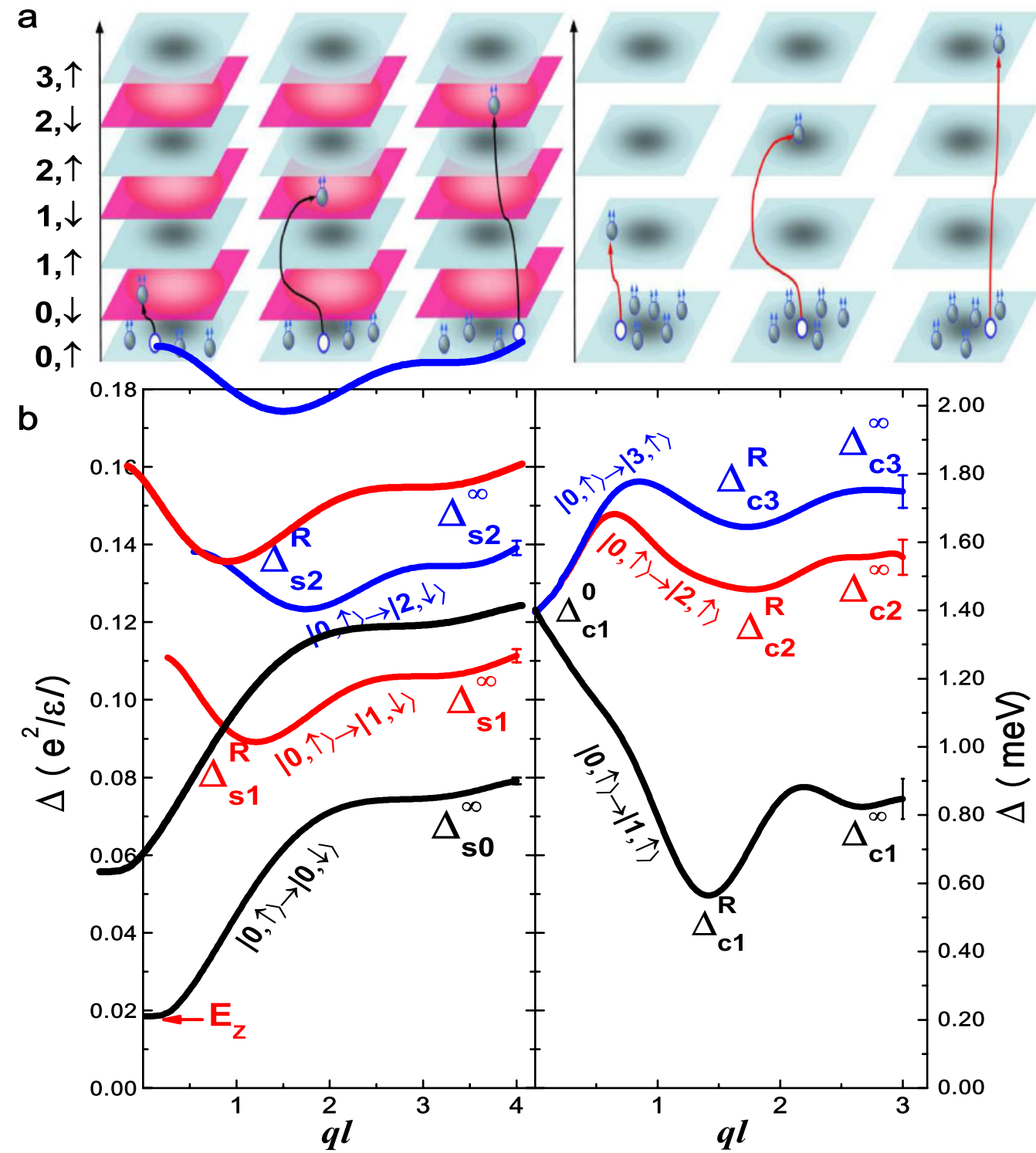


FIG. 3 (color online). Schematic diagram of CF excitons accompanied by theoretical calculations of their dispersions. (a) The right panel shows pictorially the SC excitations  $|0, \uparrow\rangle \rightarrow |K, \uparrow\rangle$  across  $K$   $\Lambda$  levels. The left panel shows the spin-flip modes  $|0, \uparrow\rangle \rightarrow |K, \downarrow\rangle$  (b) Calculated dispersions of CF excitons for a 35 nm wide GaAs quantum well with an electron density of  $5.0 \times 10^{10} \text{ cm}^{-2}$ . The right (left) panel shows the dispersions for SC (SF) modes. The error bar at the end of each curve represents the typical statistical uncertainty in the energy determined by Monte Carlo method. Critical points in the dispersion are labeled.

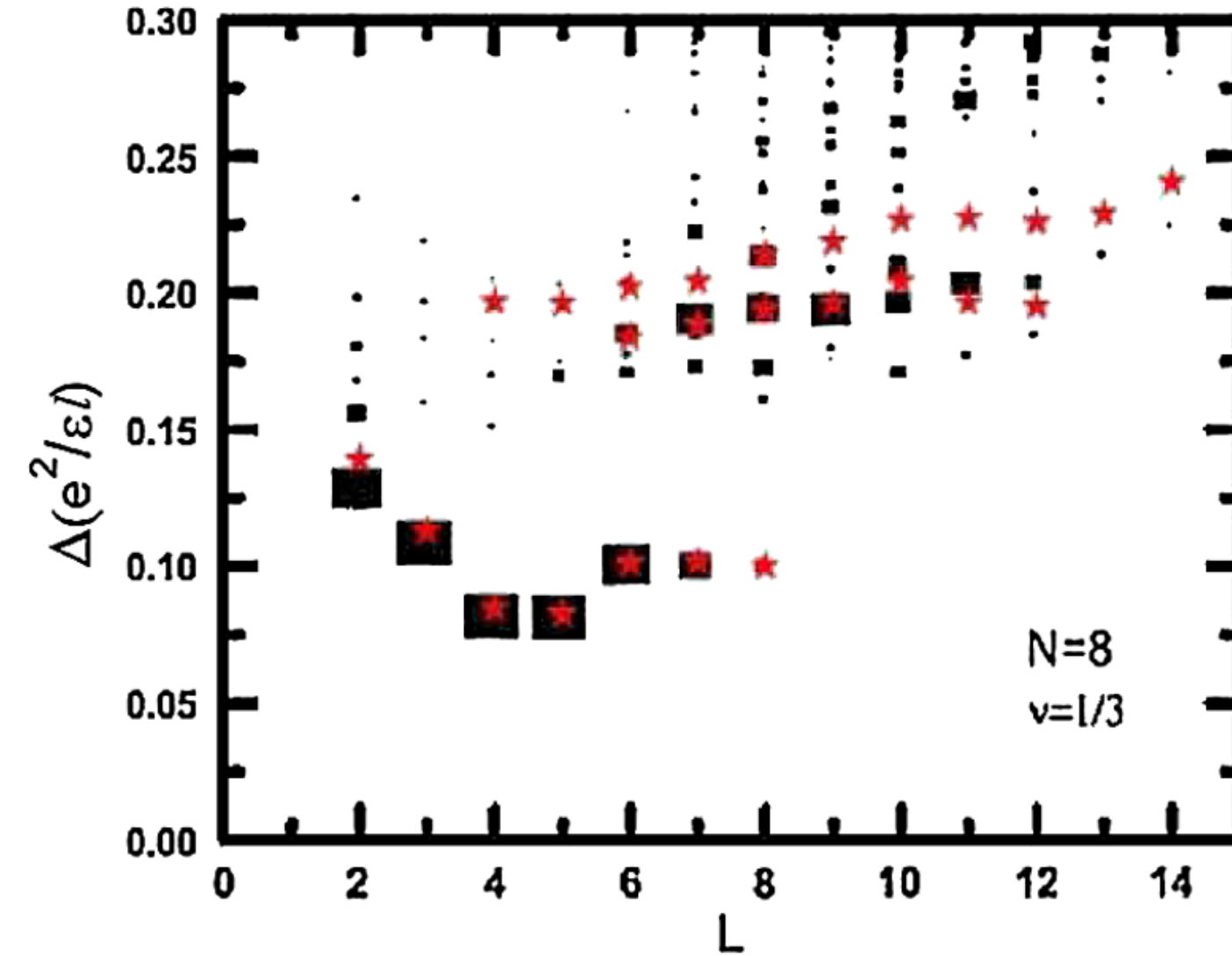


FIG. 4 (color online). Comparison of CF excitons with exact diagonalization results (in spherical geometry) for eight particles at  $\nu = 1/3$ . The (red) stars show the CF exciton dispersions for the lowest three SC branches for this system as a function of the total orbital angular momentum  $L$ . The exact spectra are taken from Ref. [12]. The area of each black rectangle is proportional to the normalized spectral weight under the state; larger spectral weight implies greater intensity in ILS. The level-1 and level-2 CF excitons closely trace lines of high spectral weight; it is possible that still higher modes will become identifiable in the exact spectra for larger systems. The other states in the exact spectrum are interpreted as made up of multiple excitons, which are expected to couple less strongly to light.

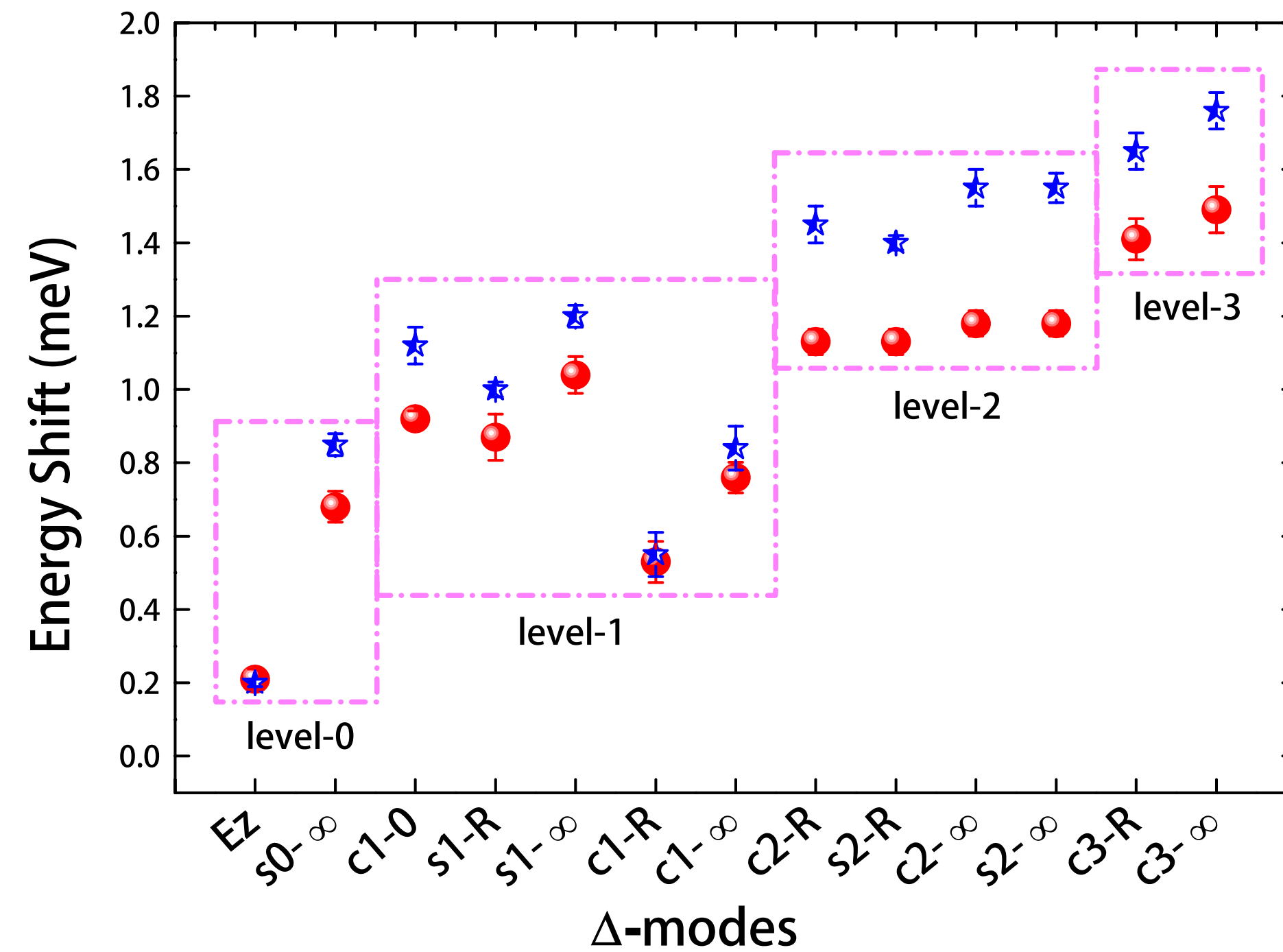


FIG. 5 (color online). Comparison between experimental energies [from Fig. 2, (red) circles] with theoretical CF exciton energies [from Fig. 3, (blue) stars], organized according to the level of the excitation. The identification of experimental modes is explained in the text. The discrepancy between theory and experiment, less than 0.2–0.3 meV, is presumably due to disorder. Estimated error bars for the experimental values are shown, unless smaller than the symbol size.

- Both theory and experiments have lots of modes. There is an approximate correspondence between their energies.

**Spin rotons**

## Observation of Nonconventional Spin Waves in Composite-Fermion Ferromagnets

U. Wurstbauer,<sup>1,\*</sup> D. Majumder,<sup>2</sup> S. S. Mandal,<sup>2</sup> I. Dujovne,<sup>3</sup> T. D. Rhone,<sup>1</sup> B. S. Dennis,<sup>4</sup> A. F. Rigosi,<sup>1</sup> J. K. Jain,<sup>5</sup>  
A. Pinczuk,<sup>1,6</sup> K. W. West,<sup>7</sup> and L. N. Pfeiffer<sup>7</sup>

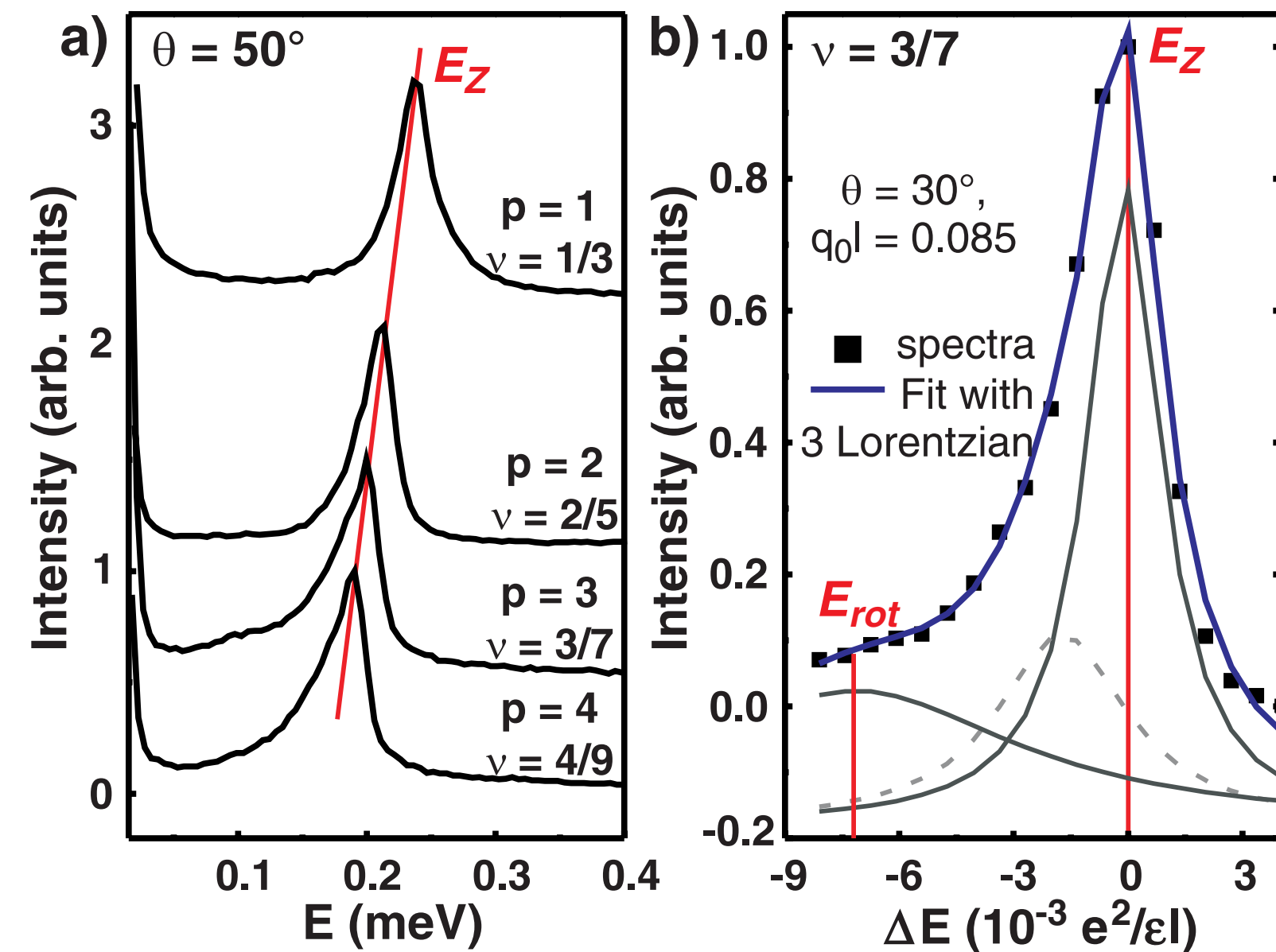
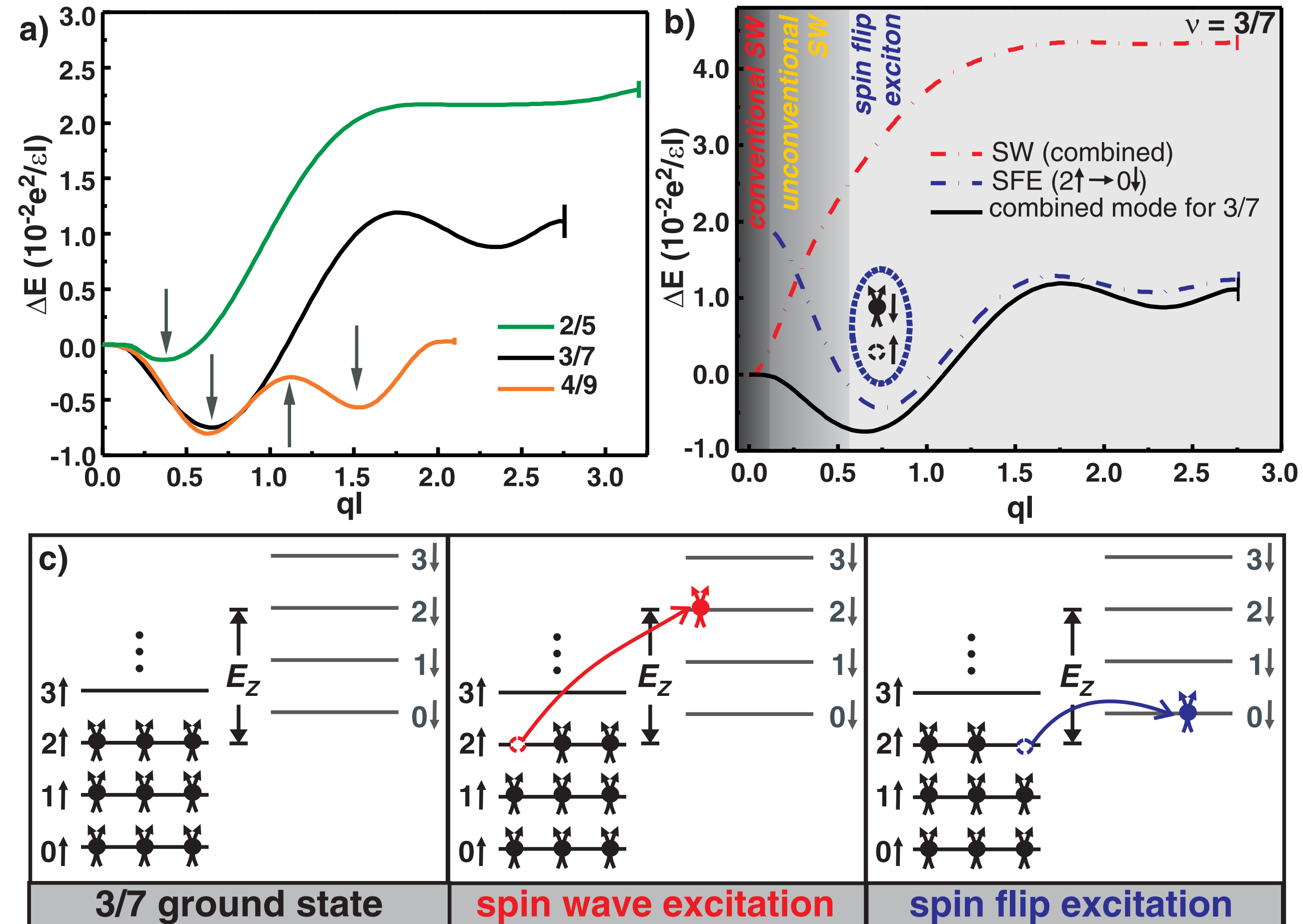


FIG. 2 (color online). Inelastic light scattering spectra in the energy range of lowest spin-reversed excitations. (a) Results for  $1/3 \leq \nu \leq 4/9$  ( $1 \leq p \leq 4$ ) at  $\theta = 50^\circ$ . The tail below  $E_Z$  increases with increasing  $\Lambda L$  number  $p$ . At  $\nu = 1/3$  only a high energy tail is observable. (b) Spectra at  $\nu = 3/7$  for  $\theta = 30^\circ$  (black squares). The black (blue) line is a fit with three individual Lorentzians shown in gray. The peak positions are marked with vertical lines.

- Experiments show spin flip modes below the Zeeman energy at  $\nu = 2/5, 3/7, 4/9$ !



- The spin wave is renormalized by the spin-flip CF exciton that alters the CF-LL Index. This produces sub-Zeeman spin rotons at  $2/5, 3/7, \dots$
- No sub-Zeeman spin roton is expected at  $1/3$ .

# Quantitative comparisons with experiment

TABLE I. Momenta and energies of rotons and maxons modes from calculation and from Lorentzian fits to the experiment for both  $\theta = 30^\circ$  and  $50^\circ$ .

$\nu$	Mode	$ql$	$\Delta E_{\text{theory}}$ $10^{-3}(e^2/\epsilon l)$	$\Delta E_{30^\circ}$ $10^{-3}(e^2/\epsilon l)$	$\Delta E_{50^\circ}$ $10^{-3}(e^2/\epsilon l)$
2/5	$E_{\text{rot}}$	0.373	-1.39	-0.98	-1.49
3/7	$E_{\text{rot}}$	0.638	-7.48	-7.43	-6.20
4/9	$E_{\text{rot}}^1$	0.63	-8.05	-6.20	-7.20
	$E_{\text{max}}$	1.134	-2.96	-2.80	-3.20
	$E_{\text{rot}}^2$	1.533	-5.69		

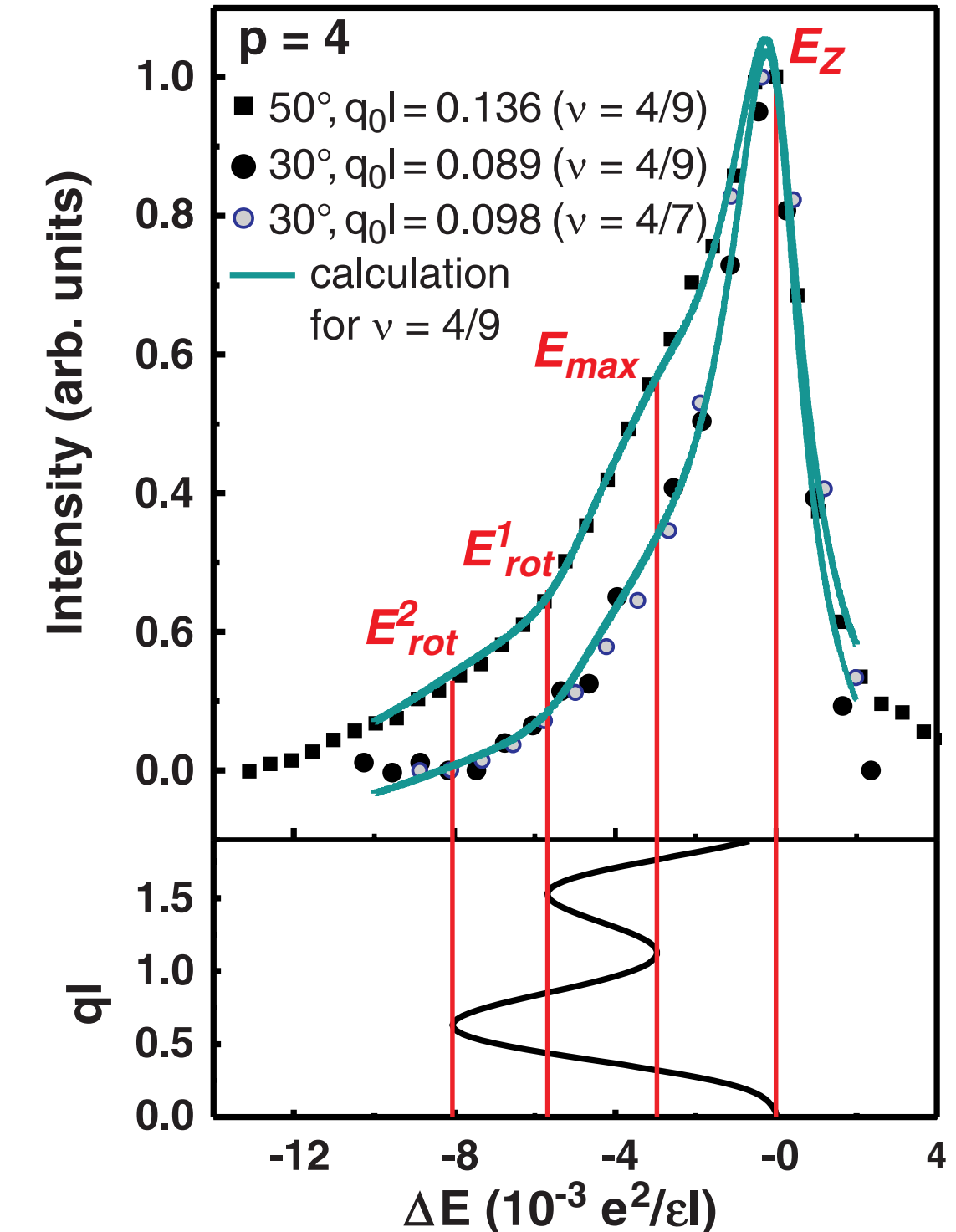


FIG. 4 (color online). Upper panel: Spectra at  $\nu = 4/9$  for  $\theta = 50^\circ$  (solid squares) and  $\theta = 30^\circ$  (solid circles) and at  $\nu = 4/7$  for  $\theta = 30^\circ$  (open blue circles). The solid lines are calculated ILS intensities for  $\nu = 4/9$  at  $\theta = 50^\circ$  and  $30^\circ$ . Lower panel: Calculated wave vector dispersion for  $\nu = 4/9$ .

- An excellent qualitative and quantitative understanding of the sub-Zeeman spin rotons has been achieved.

**CF skyrmions**

## Evidence of Landau Levels and Interactions in Low-Lying Excitations of Composite Fermions at $1/3 \leq \nu \leq 2/5$

Irene Dujovne,<sup>1,2</sup> A. Pinczuk,<sup>1,2,3</sup> Moonsoo Kang,<sup>1,2</sup> B. S. Dennis,<sup>2</sup> L. N. Pfeiffer,<sup>2</sup> and K. W. West<sup>2</sup>

<sup>1</sup>Department of Applied Physics and Applied Math, Columbia University, New York, New York 10027

<sup>2</sup>Bell Labs, Lucent Technologies, Murray Hill, New Jersey 07974

<sup>3</sup>Department of Physics, Columbia University, New York, New York 10027

(Received 2 August 2002; published 23 January 2003)

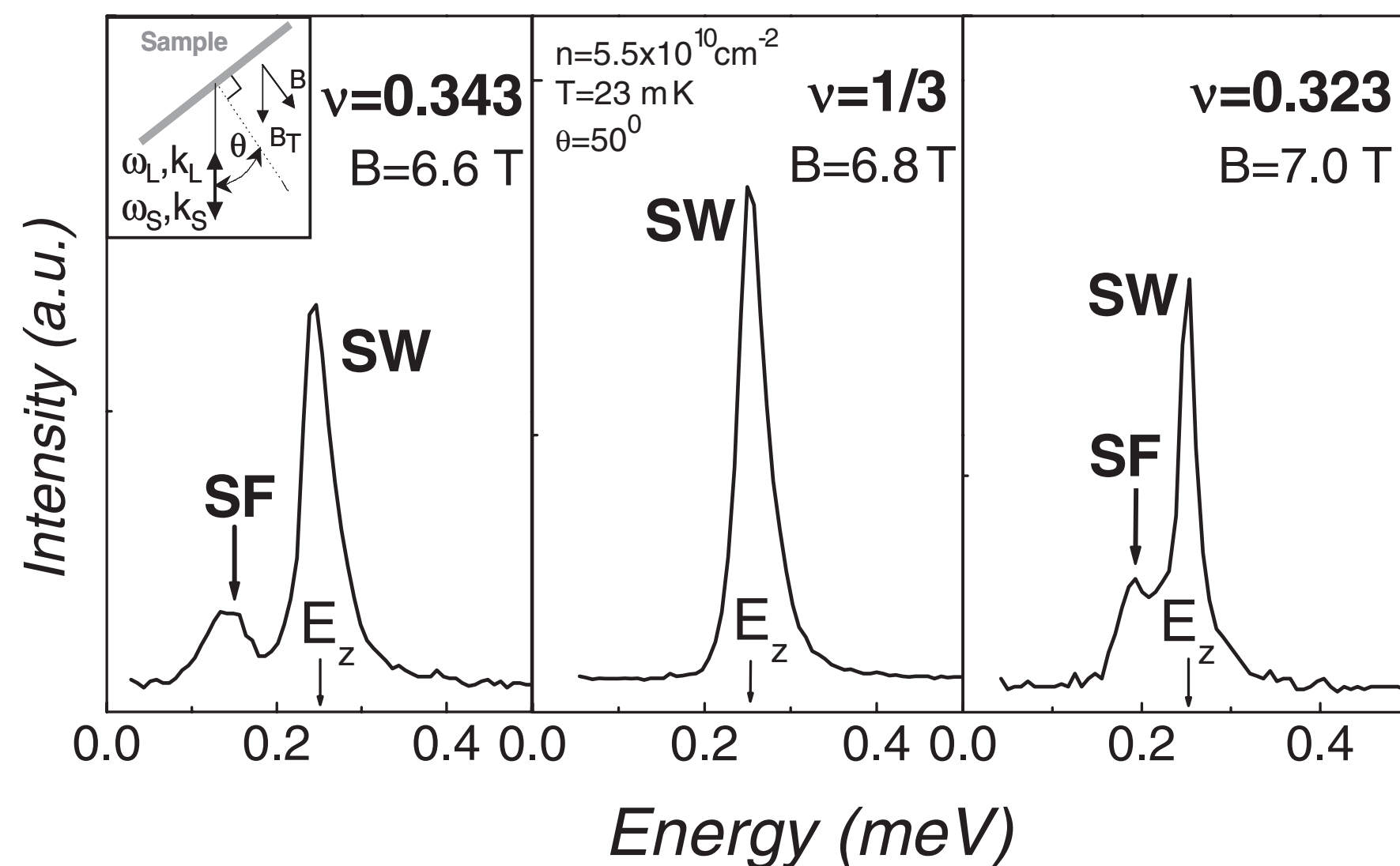


FIG. 2. Light scattering spectra of the low-lying spin excitations at three different filling factors:  $\nu = 0.343$ ,  $\nu = 1/3$ , and  $\nu = 0.323$ . The scattering geometry is shown in the inset.

## Transition from Free to Interacting Composite Fermions away from $\nu = 1/3$

Y. Gallais,<sup>1,\*</sup> T. H. Kirschenmann,<sup>1</sup> I. Dujovne,<sup>1,†</sup> C. F. Hirjibehedin,<sup>1,‡</sup> A. Pinczuk,<sup>1,2</sup>  
B. S. Dennis,<sup>2</sup> L. N. Pfeiffer,<sup>2</sup> and K. W. West<sup>2</sup>

<sup>1</sup>Departments of Physics and of Applied Physics, Columbia University, New York, New York 100, USA

<sup>2</sup>Bell Labs, Lucent Technologies, Murray Hill, New Jersey 07974, USA

(Received 2 May 2006; published 19 July 2006)

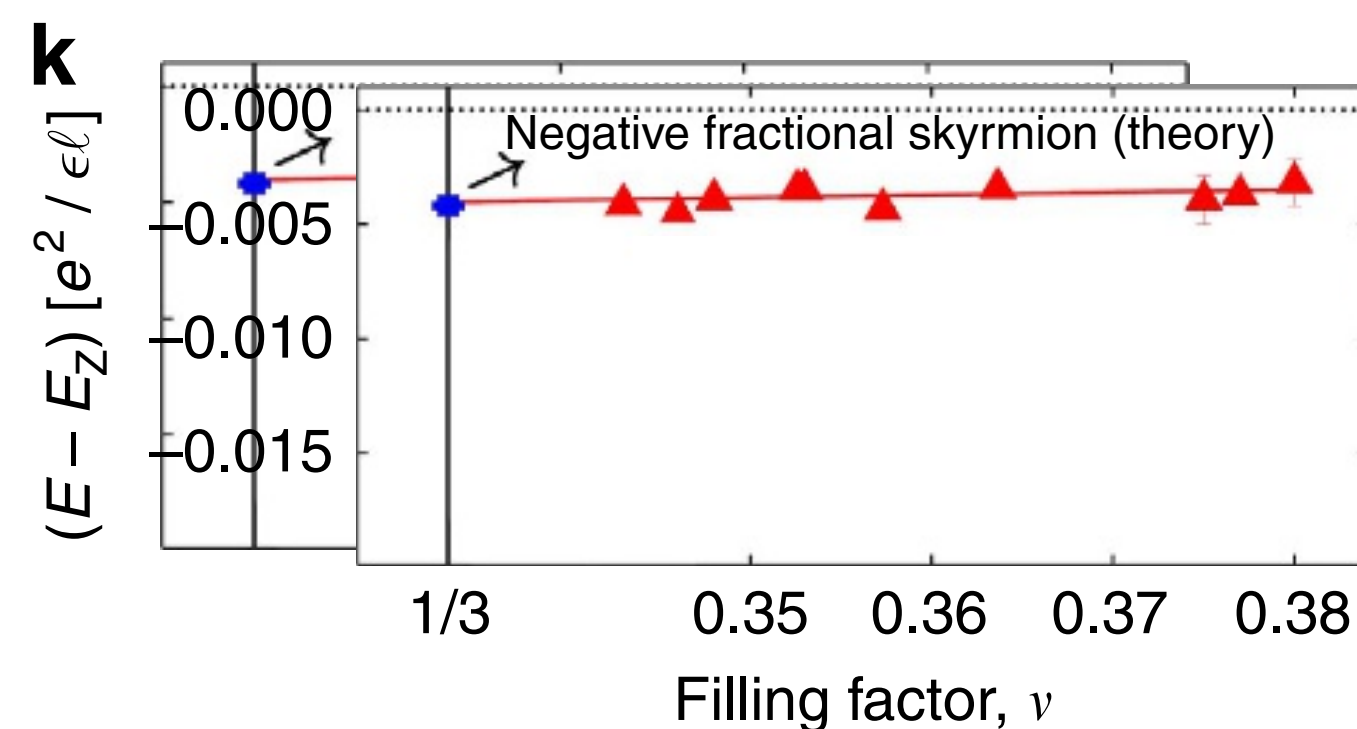
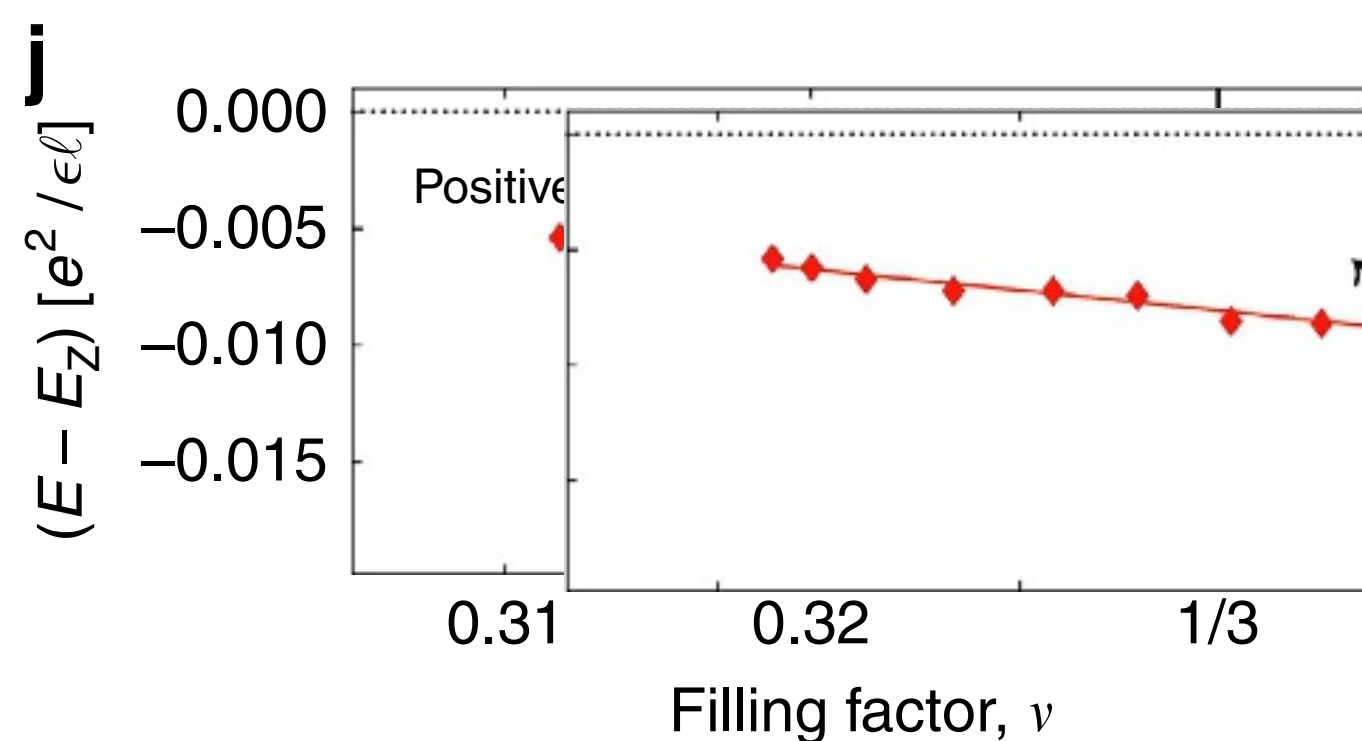
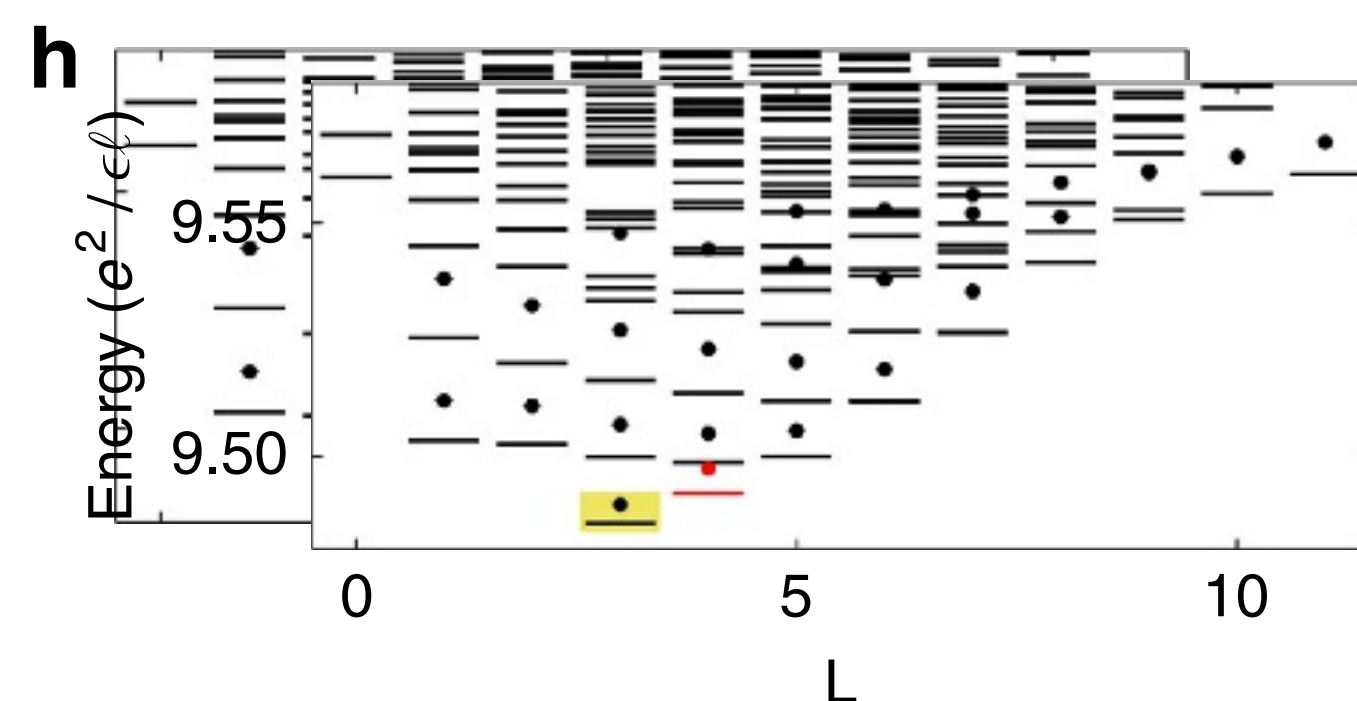
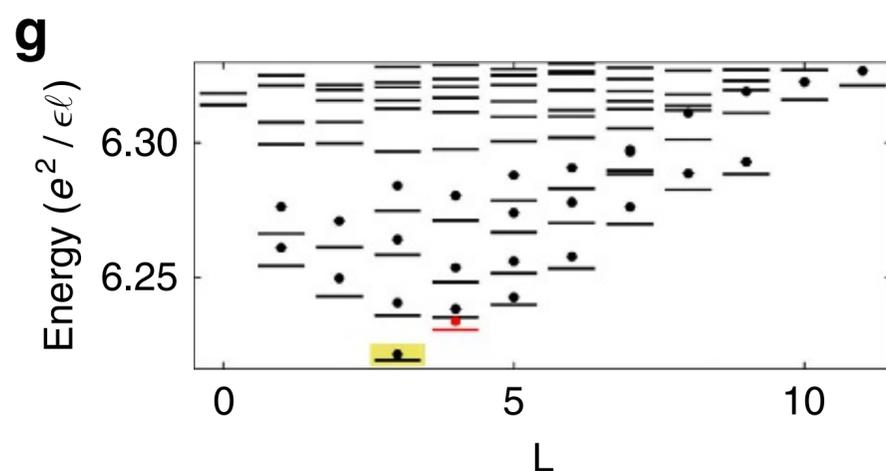
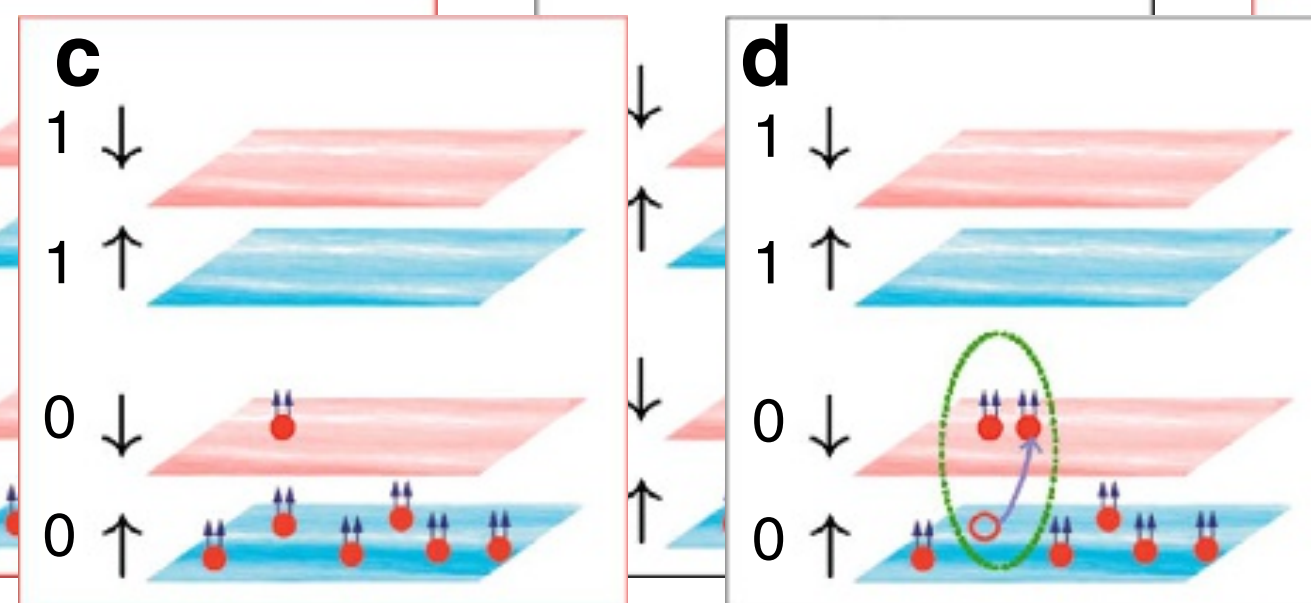
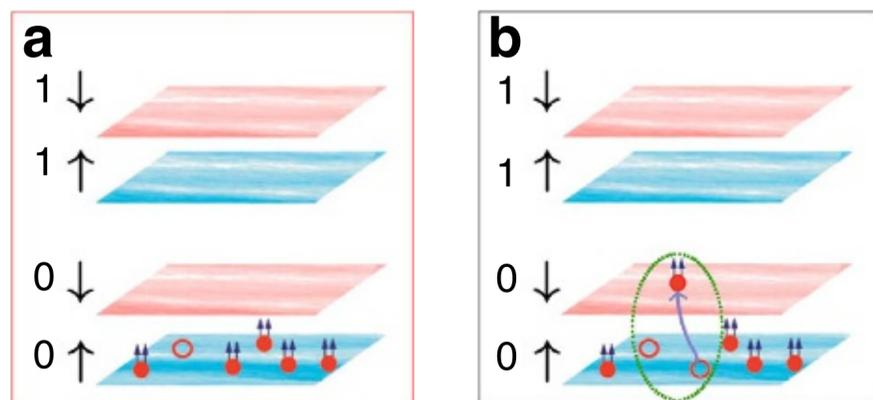
- At  $\nu = 1/3$ , there is no sub-Zeeman mode.
- For  $\nu > 1/3$  and  $\nu < 1/3$  there are sub-Zeeman modes.

# Fractionally charged skyrmions in fractional quantum Hall effect

Ajit C. Balram<sup>1</sup>, U. Wurstbauer<sup>2,3</sup>, A. Wójs<sup>4</sup>, A. Pinczuk<sup>5</sup> & J.K. Jain<sup>1</sup>

**Positively charged CF skyrmion  $\nu < 1/3$  ( $\nu^* < 1$ )**

**Negatively charged CF skyrmion  $\nu > 1/3$  ( $\nu^* > 1$ )**



- The sub-Zeeman excitations are the tiniest avatars of skyrmions (i.e., CF quasiparticles or CF quasiholes dressed by a single spin-flip CF exciton). These have positive charge for  $\nu < 1/3$  ( $\nu^* < 1$ ), and negative for  $\nu > 1/3$  ( $\nu^* > 1$ ).
- This provides an excellent quantitative account of experiment.
- For sufficiently small Zeeman splittings, a QH or QP will spontaneously bind one or many spin-flip excitons.

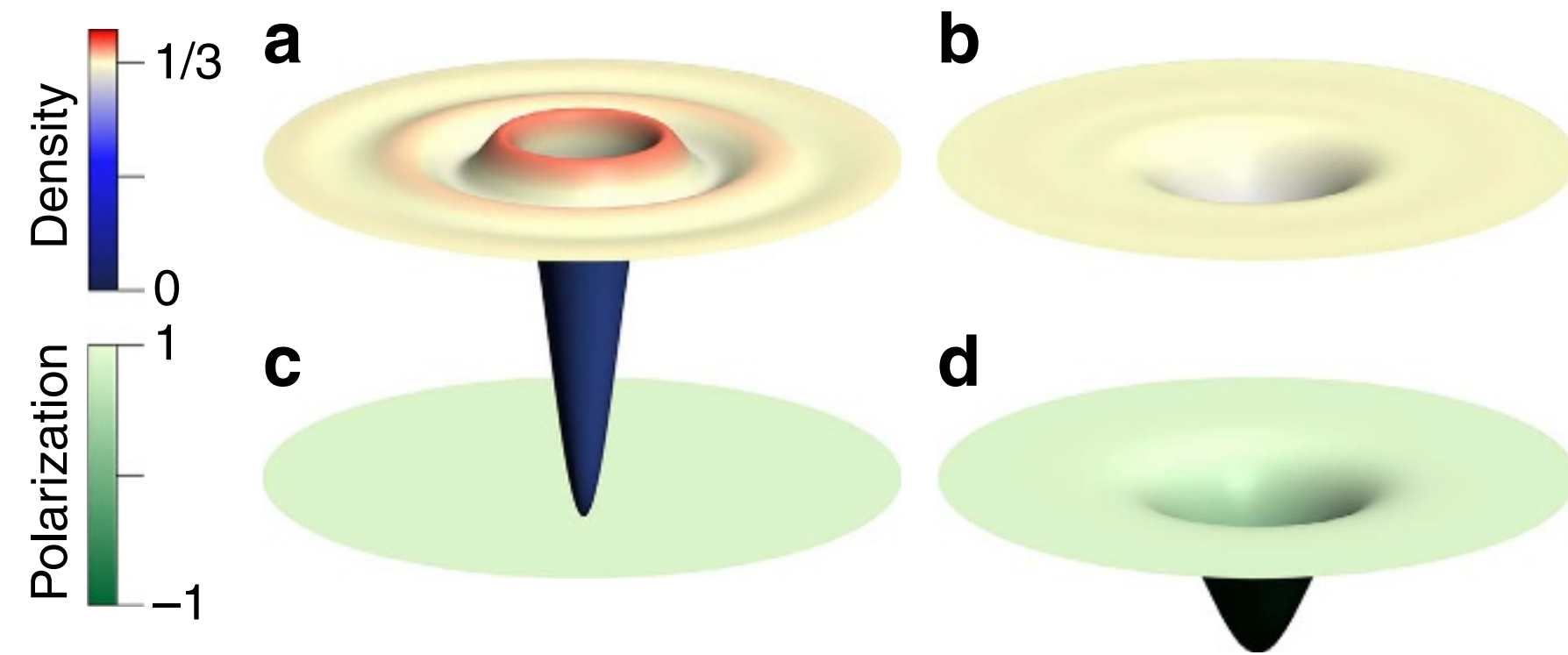


**Figure 3 | Contrasting the positively charged skyrmion with the composite fermion (CF) hole.** (a,b) show charge density profiles of a CF hole and a positively charged fractional skyrmion. Their spin polarization, defined by  $(\rho_{\uparrow}(r) - \rho_{\downarrow}(r)) / (\rho_{\uparrow}(r) + \rho_{\downarrow}(r))$  where  $\rho_{\uparrow}(r)$  and  $\rho_{\downarrow}(r)$  are the spatial densities of spin-up and spin-down composite fermions, is shown in c,d, respectively. The minimum/maximum values of the colour bars in each panel are: (a) 0.006/0.357, (b) 0.266/0.333, (c) 1.000/1.000, (d)  $-0.695/1.000$ . The disk shown has a radius of  $12.5 \ell$ .

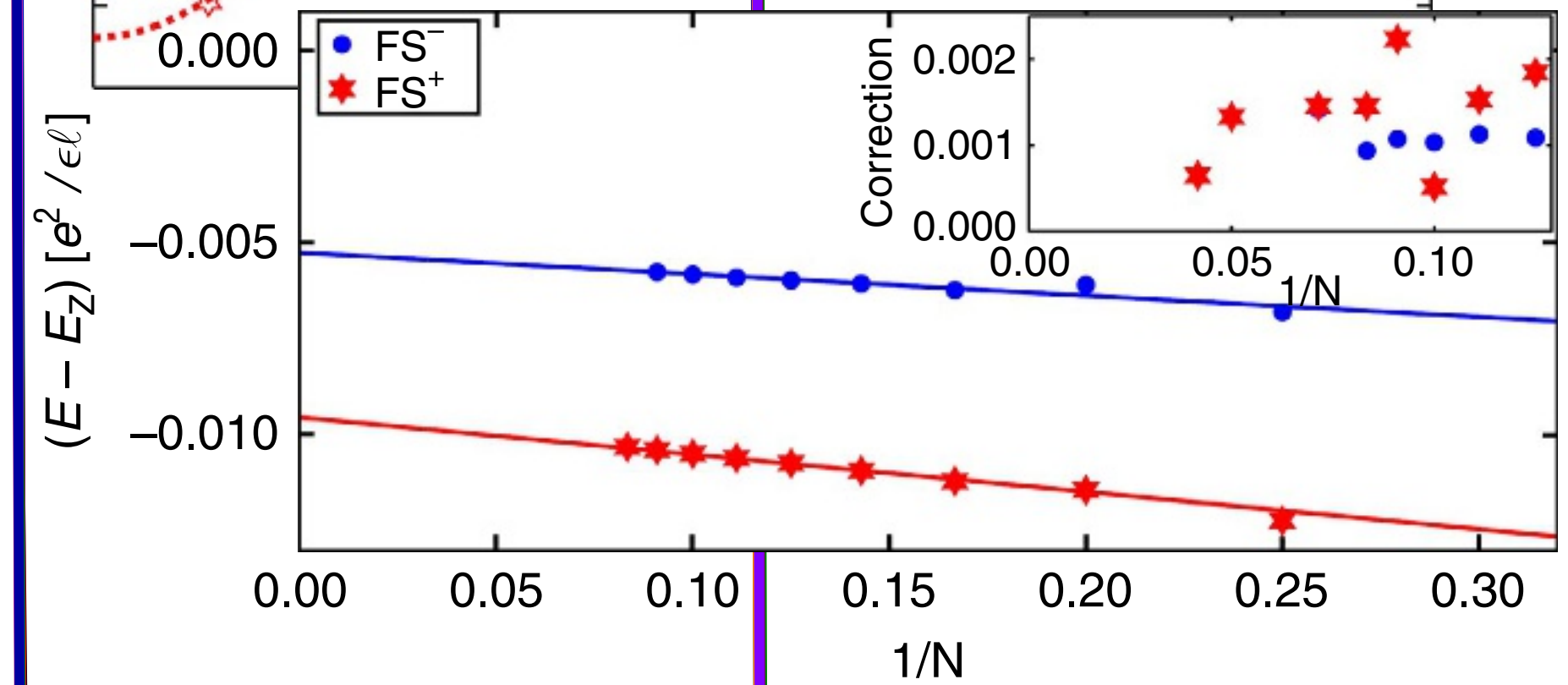
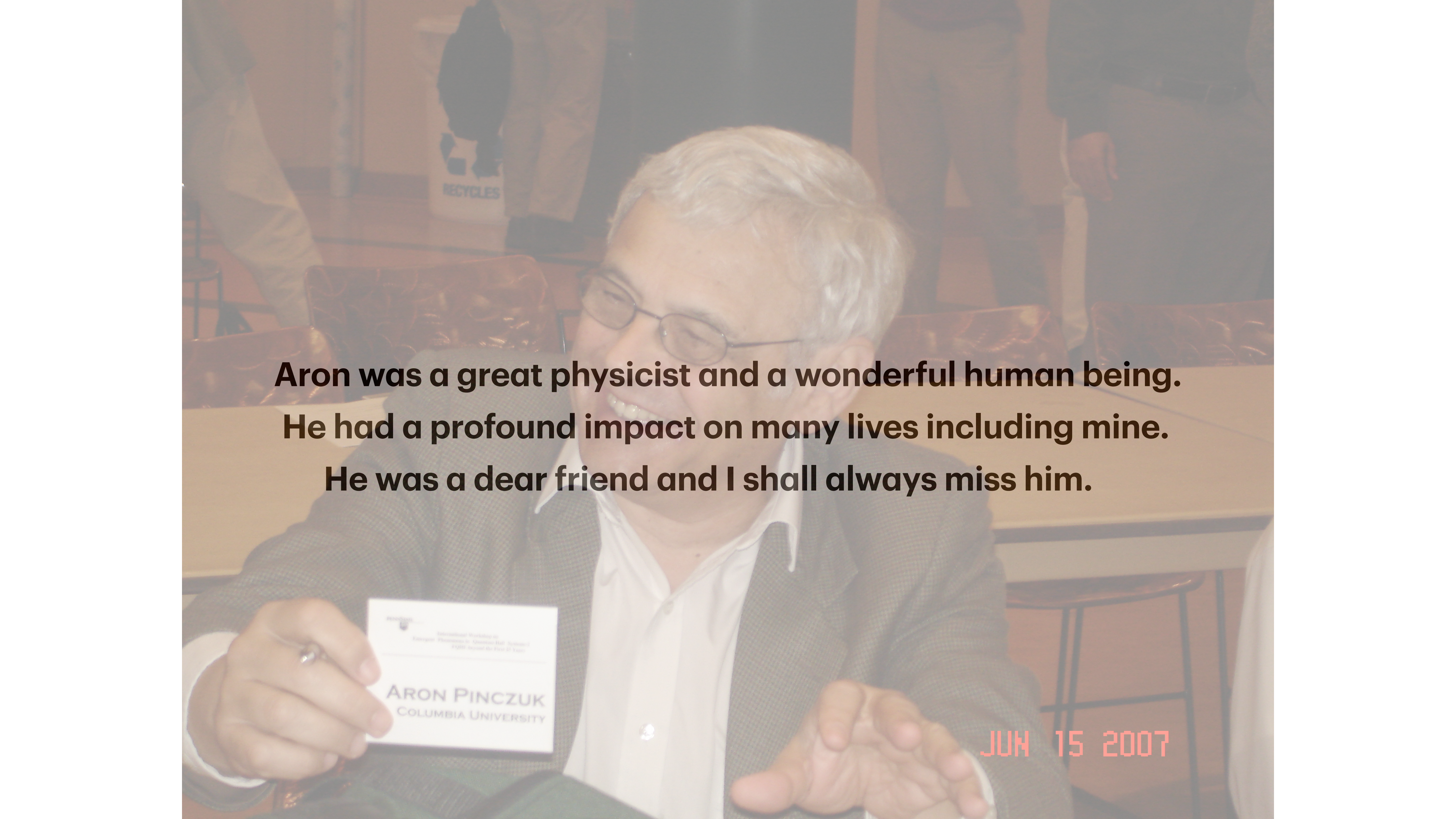


**Figure 4 | Thermodynamic extrapolation of the binding energies of the fractional skyrmions.** The blue (red) symbols show the energies of negative (positive) fractional skyrmions for a system of  $N$  particles with zero transverse width, obtained from exact diagonalization. The inset shows the amount by which finite-width corrections lower the energy of the fractional skyrmion (FS) for a sample of width 33 nm.



**Aron was a great physicist and a wonderful human being.  
He had a profound impact on many lives including mine.  
He was a dear friend and I shall always miss him.**

JUN 15 2007